Event-Triggered and Intermittent Emulation of Safety-Critical Controllers for Nonlinear Systems

Lijun Long, Zhongkui Zhang, and Zhiyong Chen

***Abstract*—This paper explores the emulation of safety-critical controllers for nonlinear systems within the constraints of limited computational resources and system data. We introduce innovative dynamic event-triggered and intermittent control strategies to digitally implement any given safety-critical controller constructed using a high-order control barrier function and its resultant Lyapunov function. These strategies simultaneously ensure forward invariance, asymptotic convergence, and prevent the Zeno phenomenon while providing an explicit characterization of the minimal dwell time. Our approach offers significant advantages in terms of resource efficiency compared to continuous-time safety-critical controllers. Additionally, we develop an extended framework to address the same control problem in the presence of unknown dynamics, enabling the application of a learning-based approach. We illustrate the effectiveness of the proposed design strategies through both an academic example and a practical problem in adaptive cruise control.**

***Index Terms*—Nonlinear Systems, Safety-critical control, Event-triggered control, Intermittent control.**

I. Introduction

Ensuring real-time safety is of paramount concern in the realm of safety-critical systems, spanning domains such as self-driving cars, autonomous mobile robots, industrial manipulators, and chemical reactors [1], [2], [3]. The violation of safety constraints can lead to significant damage in various scenarios [4], [5], [6], [7], [8]. Consequently, the pursuit of provable safety-critical control for dynamical systems has garnered substantial attention within the control systems community. A common formulation of real-time safety in control design revolves around ensuring that system states remain confined within a predefined forward-invariant space. This type of control design is commonly referred to as safety-critical control.

Such control designs have found widespread and successful application in nonlinear systems through the utilization of a control barrier function (CBF) [9], [10]. However, most existing results are predicated on the assumption that the relative degree of the system concerning a function enforcing a safety constraint is one. Recently, [11], [12], [13] extended a CBF to a high-order control barrier function (HOCBF), which can accommodate high relative degree constraints. These designs, along with others such as those in [10], [14], can achieve closed-loop safety-critical systems, albeit they must be implemented in a continuous-time fashion.

In many modern control applications, designing a real-time controller necessitates the consideration of several factors, including computational resource constraints and actuator limitations. Therefore, researchers have extensively investigated event-triggered control (ETC) schemes, wherein data transmission and control updates occur only when an event generated by a predefined event-triggered mechanism (ETM) occurs. Most recent efforts have been dedicated to developing systematic approaches for designing ETMs [15], [16], [17], [18], [19]. The motivation behind this paper is to investigate the digital emulation of the most advanced safety-critical controllers, using HOCBF, and propose effective event-triggered and intermittent mechanisms.

Some attempts at event-triggered safety-critical control can be found in the literature. For instance, methods aiming to achieve event-triggered safety and/or stability in nonlinear systems using an input-to-state safe (ISSf) barrier function can be found in [20], [21], along with appropriate static or dynamic ETMs. Additionally, in [22], an intermittent control scheme was developed that allows for intermittent control deactivation. However, these methods require the measurement error caused by the ETM to satisfy certain input-to-state stable (ISS) and/or ISSf assumptions for the closed-loop systems. Moreover, in [20], an explicit lower bound for the minimal dwell time cannot be obtained. In [21], an additional assumption of a bounded constraint on the system nonlinearity is introduced to ensure a strictly positive lower bound on inter-event times. Importantly, all the mentioned results implicitly assume that the safety function's relative degree with respect to the control input is one.

Motivated by these limitations in existing attempts, this paper aims to explore event-triggered and intermittent mechanisms in a more general setting. Specifically, we propose novel and structurally simple dynamic ETMs using an HOCBF and its resultant Lyapunov function to achieve forward invariance, asymptotic convergence, and the avoidance of the Zeno phenomenon, thus relaxing the aforementioned limitations found in the literature.

Furthermore, due to parametric uncertainties and unmod-

This work was supported by the National Natural Science Foundation of China under Grant 62173075 and Grant 61773100, the 111 Project under Grant B16009, and the LiaoNing Revitalization Talents Program under Grant XLYC1907043, and the Fundamental Research Funds for the Central Universities under Grant N25BSS037 and Grant N25DCG005. (Corresponding author: Lijun Long.)

L. Long is with the College of Information Science and Engineering, Northeastern University, Shenyang, 110819, China, and with the State Key Laboratory of Synthetical Automation for Process Industries, Northeastern University, Shenyang, 110819, China, and also with the Key Laboratory of Data Analytics and Optimization for Smart Industry (Northeastern University), Ministry of Education, China. Z. Zhang is with the Shenyang Institute of Automation, Chinese Academy of Sciences, Shenyang, 110016, China. Z. Chen is with the School of Engineering, The University of Newcastle, Callaghan, NSW 2308, Australia. (e-mail: longlijun@ise.neu.edu.cn, long_lijun@126.com (L. Long), zack_zhang2019@126.com (Z. Zhang), zhiyong.chen@newcastle.edu.au (Z. Chen)).

eled dynamics, the models used to design controllers are imperfect, potentially compromising the safety of a control system. This motivates us to synthesize controllers capable of handling model uncertainty. In safety-critical control, some learning frameworks that address model uncertainty have been proposed in [23], [24]. To the best of our knowledge, only a few works, such as [25], [26], have considered the same problem in an event-triggered fashion based on HOCBFs. These approaches employ adaptive affine control, updated based on error states, to approximate unmodeled system dynamics.

However, the design in [25], [26] employs a fixed threshold event-triggered mechanism based on state and error bounds, which may result in excessive control frequency. Additionally, the trigger mechanism designed for HOCBFs is relatively complex, and the controller optimized for worst-case performance may not fully exploit the advantages of controller performance. In this paper, we further develop a supervised learning framework to address the issue of unknown dynamics in the proposed event-triggered and intermittent mechanisms, thereby overcoming the limitations found in the existing literature.

In summary, the contribution of our work is listed below.

(i) The proposed event-triggered and intermittent mechanisms enable the successful emulation of safety-critical controllers, significantly reducing the unnecessary consumption of communication and actuation resources. Compared to existing results, such as those in [25], [26], the designed event-triggered mechanism features a simple structure with high computational efficiency. It ensures the safety and asymptotic stability of the system under an HOCBF constraint.

(ii) The proposed method allows for the removal of the additional ISSf barrier function or ISS Lyapunov function assumptions employed in [20], [21]. Additionally, it provides an explicit characterization of the minimal dwell time to prove the avoidance of the Zeno phenomenon.

(iii) We generalize our method to unknown nonlinear systems using supervised learning methods (e.g., Neural Networks) under high-order constraints, framing the design within the realm of intelligent optimization.

The rest of this paper is organized as follows. Section II provides the problem description and preliminaries. The main results of this paper regarding event-triggered emulation and intermittent emulation are presented in Section III and Section IV, respectively. The method is extended to handle unknown system dynamics in Section V. Two illustrative examples are provided in Section VI. Conclusions are drawn in Section VII.

Notations: Let $\mathbb{R}_{\geq 0} = [0,\infty)$, $\mathbb{R}_{>0} = (0,\infty)$, and $\mathbb{N}$ denotes the set of non-negative integers. The Euclidean norm is denoted by $\|\cdot\|$. A continuous function $\alpha : [0,a) \to [0,\infty)$ for some $a > 0$ is of class $\mathscr{K}$ if it is strictly increasing, and $\alpha(0) = 0$. If $a = \infty$ and $\lim_{r\to\infty} \alpha(r) = \infty$, then α is of class $\mathscr{K}_\infty$. A continuous function $\alpha : (-b,a) \to \mathbb{R}$ with $a,b > 0$ is of extended class $\mathscr{K}$ if $\alpha(0) = 0$, and α is strictly monotonically increasing. If $a,b = \infty$, $\lim_{r\to\infty} \alpha(r) = \infty$, and $\lim_{r\to-\infty} \alpha(r) = -\infty$, then α is of extended class $\mathscr{K}_\infty$. The inverse of a function $\alpha : \mathbb{R} \to \mathbb{R}$ with respect to a constant ε is defined by $\alpha^{-1}(\varepsilon)$. A function $\beta : \mathbb{R}_{\geq 0} \times \mathbb{R}_{\geq 0} \to \mathbb{R}_{\geq 0}$ is of class $\mathscr{KL}$ if $\beta(\cdot,t)$ is of class $\mathscr{K}$ for each fixed $t \geq 0$, and $\beta(r,\cdot)$ decreases to 0 as $t \to \infty$ for each fixed $r \geq 0$. A function $\beta : \mathbb{R} \times \mathbb{R}_{\geq 0} \to \mathbb{R}$ is of extended class $\mathscr{K}_\infty\mathscr{L}$ if $\beta(\cdot,t)$ is of extended class $\mathscr{K}_\infty$ for each fixed $t \geq 0$, and $\beta(r,\cdot)$ decreases to 0 as $t \to \infty$ for each fixed $r \geq 0$, and $\beta(r,\cdot)$ increases to 0 as $t \to \infty$ for each fixed $r < 0$. The Lie derivative of a differentiable function $h : \mathbb{R}^n \to \mathbb{R}$ along a vector field $f : \mathbb{R}^n \to \mathbb{R}^n$ is defined as $L_f h(x) = \frac{\partial h}{\partial x} f(x)$, and this notation allows us to denote higher-order Lie derivatives along an additional vector field g as $L_f^i h(x) = \frac{\partial (L_f^{i-1} h)}{\partial x} f(x)$ and $L_g L_f^{i-1} h(x) = \frac{\partial (L_f^{i-1} h)}{\partial x} g(x)$. For a closed set $\mathscr{S}$, let $\partial\mathscr{S}$ and Int$\mathscr{S}$ be the boundary and interior, respectively.

II. Problem Formulation and Preliminaries

Consider a nonlinear control system of the affine form:

$$\dot{x} = f(x) + g(x)u, \tag{1}$$

where $x \in \mathbb{R}^n$ represents the system state, $u \in \mathbb{U} \subset \mathbb{R}^q$ is the control input, and $f : \mathbb{R}^n \to \mathbb{R}^n$ and $g : \mathbb{R}^n \to \mathbb{R}^{n\times q}$ are locally Lipschitz functions with $f(0) = 0$. Given a locally Lipschitz feedback law $u = k(x)$ with $k(0) = 0$, the closed-loop vector field is defined as $f_c \triangleq f(x) + g(x)k(x)$, which is also locally Lipschitz. This implies that the closed-loop system (1) admits a unique solution $x : I(x_0) \to \mathbb{R}^n$ starting from an initial state $x_0 = x(t_0) \in \mathbb{R}^n$ on a maximal interval of existence $I(x_0) = [t_0, t_{\max})$. If the closed-loop system (1) is forward complete, then $t_{\max} = \infty$.

Let $\mathscr{S} \subset \mathbb{R}^n$ be a nonempty simply-connected set without isolated points, and assume that $0 \in \mathscr{S}$. Safety-critical control for the system (1) with respect to $\mathscr{S}$ has been extensively studied in the literature [9], [11], [20], [27]. This approach aims to design a closed-loop system that admits a forward-invariant set $\mathscr{S}$, which is defined as follows.

Definition 2.1: The set $\mathscr{S} \subset \mathbb{R}^n$ is forward-invariant for the system (1) with $u = k(x)$ if for every $x_0 \in \mathscr{S}$, the solution $x(t)$ satisfies $x(t) \in \mathscr{S}$ for all $t \in I(x_0)$.

Remark 2.1: In the literature, the closed-loop system (1) with $u = k(x)$ is commonly referred to as 'safe' with respect to the set $\mathscr{S}$ when $\mathscr{S}$ is forward-invariant for the system. In this context, the set $\mathscr{S}$ is often called a safe set.

In the realm of control system design, there exists a method for crafting a continuous-time controller denoted as $u = k(x)$ to achieve a forward-invariant set $\mathscr{S}$. This method, rooted in the concept of HOCBF, has been extensively explored in the literature, with references including [11], [28], [29]. To comprehensively understand the HOCBF framework, we first introduce the definition of relative degree along with some notations. Denote $g(x) = [g_1(x), \ldots, g_q(x)]$ and $u = [u_1, \ldots, u_q]^T$.

Definition 2.2: [30] The single-input single-output system

$$\dot{x} = f(x) + g_l(x)u_l,\ y = h(x) \tag{2}$$

for a (sufficiently) differentiable function $h : \mathbb{R}^n \to \mathbb{R}$, is said to have relative degree m at a point x^* if $L_{g_l} L_f^i h(x) = 0$ for all x in a neighborhood of x^* and all $i < m-1$, and $L_{g_l} L_f^{m-1} h(x^*) \neq 0$.

Remark 2.2: In Definition 2.2, the value m is also called the relative degree of the function h with respect to the system (2).

In the literature studying HOCBF, e.g., [11], a more general definition of relative degree for $h(x)$ is adopted, which holds globally for $x \in \mathbb{R}^n$ and for all multiple inputs. Specifically, h has relative degree m with respect to the system (1) if $L_g L_f^i h(x) = 0$ for all $i < m-1$ and $L_g L_f^{m-1} h(x) \neq 0$, for all $x \in \mathbb{R}^n$. This essentially means that the relative degree m is the number of times we need to differentiate $h(x)$ along (1) until the control u explicitly appears.

In this paper, since the function h is used to define a constraint $h(x) \geq 0$, we can also refer to the relative degree of h as the relative degree of the constraint. For any differentiable extended class $\mathscr{K}_\infty$ functions $\alpha_i(\cdot)$, $i \in \{1,\ldots,m\}$, and a C^m function h of relative degree m for the system (1), we define a sequence of functions along the system trajectory as follows:

$$\begin{aligned} \psi_0(x) &= h(x), \\ \psi_i(x) &= \dot{\psi}_{i-1}(x) + \alpha_i\big(\psi_{i-1}(x)\big),\ i \in \{1,\ldots,m-1\}, \\ \psi_m(x,u) &= \dot{\psi}_{m-1}(x) + \alpha_m\big(\psi_{m-1}(x)\big). \end{aligned} \tag{3}$$

Consequently, this leads to a sequence of sets

$$\mathscr{C}_i = \{x \in \mathbb{R}^n : \psi_{i-1}(x) \geq 0\},\ i \in \{1,\ldots,m\}. \tag{4}$$

The time derivatives in (3) can be explicitly expressed as:

$$\dot{\psi}_{i-1}(x) = \frac{d\psi_{i-1}(x)}{dt} = L_f^i h(x) + O_{i-1}(x),\ i \in \{1,\ldots,m-1\},$$
$$\dot{\psi}_{m-1}(x) = \frac{d\psi_{m-1}(x)}{dt} = L_f^m h(x) + L_g L_f^{m-1} h(x) u + O_{m-1}(x),$$

where $O_{i-1}(x) = \sum_{j=1}^{i-1} L_f^j \left(\alpha_{i-j} \circ \psi_{i-j-1}\right)(x)$. It is noted that $\dot{\psi}_{i-1}(x)$ depends on x for $i \in \{1,\ldots,m-1\}$, whereas $\dot{\psi}_{m-1}(x)$ depends on both x and u. It is assumed that 0 is a regular value of each ψ_i, $i \in \{0,\ldots,m-1\}$, that is, $\frac{\partial \psi_i}{\partial x}(x) \neq 0$ when $\psi_i(x) = 0$ [31]. Now, the function h is termed an HOCBF if the functions $\alpha_i, i \in \{1,\ldots,m\}$ exist such that

$$\sup_{u \in \mathbb{U}} \psi_m(x,u) \geq 0,\ \ \forall x \in \mathscr{C}_1 \cap \cdots \cap \mathscr{C}_m. \tag{5}$$

With an HOCBF h in hand, we can define a set of control as:

$$K_{hocbf}(x) = \Big\{u \in \mathbb{U} : \psi_m(x,u) \geq 0\Big\}.$$

The practical application of this concept culminates in the construction of a safety-critical controller. The formal result is encapsulated in the following theorem, as cited from Theorem 4 in [11].

Theorem 2.1: Given an HOCBF h for the system (1) with the sets $\mathscr{C}_i, i \in \{1,\ldots,m\}$ defined by (4), the set $\mathscr{S} = \mathscr{C}_1 \cap \cdots \cap \mathscr{C}_m$ is forward-invariant for the system (1) with any Lipschitz continuous controller $u = k(x) \in K_{hocbf}(x)$.

In this paper, we aim to investigate the digital emulation of the continuous-time safety-critical controller $u = k(x)$ as presented in Theorem 2.1 in two distinct manners: the event-triggered emulation

$$u(t) = u(t_i) = k\big(x(t_i)\big),\ \ t \in [t_i, t_{i+1}), \tag{6}$$

and the intermittent emulation

$$u(t) = \begin{cases} u(t_i^{\text{on}}) = k\big(x(t_i^{\text{on}})\big), & t \in \left[t_i^{\text{on}}, t_i^{\text{off}}\right), \\ 0, & t \in \left[t_i^{\text{off}}, t_{i+1}^{\text{on}}\right), \end{cases} \tag{7}$$

where $i \in \mathbb{I}$. The time sequence $\{t_i\}_{i\in\mathbb{I}}$ or $\{t_i^{\text{on}}\}_{i\in\mathbb{I}}$, with $t_0^{\text{on}} = t_0$, represents the execution times at which the actual controller $u(t)$ of the system (1) is computed and updated. In the intermittent emulation, the controller is deactivated at $t_i^{\text{off}} > t_i^{\text{on}}$. If there exists an infinite number of executions, then $\mathbb{I} = \mathbb{N}$; and if there exists a finite number $J \in \mathbb{N}$ of executions, then $\mathbb{I} = \{0,1,\ldots,J\}$. Now, the main objective is summarized as follows.

Objective: We aim to design an event-triggered mechanism or an intermittent mechanism for generating the time sequences $\{t_i\}_{i\in\mathbb{I}}$ or $\{t_i^{\text{on}}, t_i^{\text{off}}\}_{i\in\mathbb{I}}$, respectively. These mechanisms are designed such that the system (1) with the controller (6) or (7), where $u = k(x)$ is given in Theorem 2.1, achieves the following properties:

P1: the solution $x(t)$ of the closed-loop system satisfies $x(t) \in \mathscr{S}$ for all $t \geq t_0$, where the set $\mathscr{S}$ is given in Theorem 2.1;

P2: every trajectory of the closed-loop system asymptotically converges to the origin as $t \to \infty$; and

P3: Zeno phenomenon is excluded in the sense that $t_{i+1} - t_i$ or $t_{i+1}^{\text{on}} - t_i^{\text{on}}$, $i \in \mathbb{I}$, has a positive lower bound, called a minimum inter-event time (MIET).

To achieve the aforementioned objective, we need to make some technical assumptions.

Assumption 2.1: There exists an HOCBF h for the system (1).

Assumption 2.2: There exists a control Lyapunov function (CLF) $V : \mathbb{R}^n \to \mathbb{R}_{\geq 0}$ for the system and the controller $k(x)$ in Theorem 2.1. In particular, there exist class $\mathscr{K}_\infty$ functions $\underline{\alpha}$, $\overline{\alpha}$ and α_v, such that for all $x \in \mathbb{R}^n$,

$$\begin{aligned} &\underline{\alpha}(\|x\|) \leq V(x) \leq \overline{\alpha}(\|x\|), \\ &L_f V(x) + L_g V(x) k(x) \leq -\alpha_v\big(\|x\|\big). \end{aligned} \tag{8}$$

Assumption 2.3: The control function k in Theorem 2.1 is Lipschitz in the set $\mathscr{S}$, that is,

$$\|k(x_1) - k(x_2)\| \leq L\|x_1 - x_2\|,\ \ \forall x_1, x_2 \in \mathscr{S}, \tag{9}$$

for a constant $L > 0$.

Remark 2.3: Assumption 2.1 is required for the continuous safety-critical controller, which is a prerequisite for the digital emulation studied in this paper. Assumption 2.2 essentially asks for compatibility of a CLF and a CBF, which is used in the study of nonlinear systems, as seen in references such as [32], [33]. Also, the condition (8) in Assumption 2.2 is adopted for nonlinear systems in [34]. This assumption can often be satisfied through effective continuous-time controller design approaches. In cases where this assumption is not fulfilled, a relaxed version will be discussed later in Remark 5.1 for practical implementation. Assumption 2.3 does not impose strong constraints on the control function k. In particular, it does not necessarily assume that the closed-loop system $\dot{x} = f(x) + g(x)k(x+e)$ subject to an external input e is ISS, as assumed in [20], [21], [22].

For a given compact set $\mathscr{D}$, we can define two positive constants L_1 and L_2 that characterize the boundaries of some terms involving α_m and ψ_{m-1} for $x \in \mathscr{D}$ as follows:

$$\alpha_m\big(\psi_{m-1}(x)\big) - \alpha_m\big(\psi_{m-1}(x) - \eta\big) \leq L_1\eta,$$

$$\max\left\{\psi_{m-1}(x)-\eta,\ \alpha_m(\psi_{m-1}(x))\right\}\leq L_2,\quad \forall x\in\mathscr{D},\ \eta\in[0,\psi_{m-1}(x)]. \tag{10}$$

Remark 2.4: These two constants, L_1 and L_2, will be used to derive the conditions for achieving the aforementioned objectives. It is important to note that these constants always exist for a compact set $\mathscr{D}$. In particular, it is selected as $\mathscr{D}=\mathscr{S}$ in Theorem 3.1 when $\mathscr{S}$ is assumed to be a compact set. It is determined by the intersection of $\mathscr{S}$ with a compact set in Theorems 3.2 and 4.1 when $\mathscr{S}$ is not assumed to be a compact set.

III. Event-Triggered Emulation

In this section, we study the event-triggered emulation of the safety-critical controller through the constructive design of a dynamic event-triggered mechanism (DETM). The main technical challenge is to simultaneously address the multiple properties formulated earlier while obtaining an explicit characterization of the minimal dwell time.

A. Dynamic Event-Triggered Mechanism

For the system (1) with the controller (6), we define a measurement error $e(t)$ as

$$e(t)=x(t_i)-x(t),\ \forall t\in[t_i,t_{i+1}),\ i\in\mathbb{I}. \tag{11}$$

Then, the DETM can be designed as follows

$$t_{i+1}=\inf_{t>t_i}\Big\{t\in\mathbb{R}_{\geq 0}\Big|\eta(t)+\theta_h\Big(\beta_h\alpha_m\big(\psi_{m-1}(x(t))\big)+M\gamma\big(\Phi_{m-1}\big(x(t),\eta(t)\big),t\big)-LD(x(t))\|e(t^-)\|\Big)\leq 0\Big\}, \tag{12}$$

where η is a dynamic variable satisfying

$$\dot\eta=-\delta_h\eta+\beta_h\alpha_m\big(\psi_{m-1}(x)\big)+M\gamma\big(\Phi_{m-1}(x,\eta),t\big)-LD(x)\|e\|,\ \eta(t_0)=\eta_0>0. \tag{13}$$

Here, $e(t^-)=\lim_{t\to t^-}e(t)$, which is obtained by continuously measuring $x(t)$ and comparing it with $x(t_i)$ for $t\in[t_i,t_{i+1})$. In the design, $\beta_h\in(0,1)$, θ_h, δ_h and M are some positive parameters, γ is an extended class $\mathscr{K}_\infty\mathscr{L}$ function, α_m and $\psi_{m-1}(x)$ are given in (3) and L given in (9), and the two functions Φ_{m-1} and D are defined as follows

$$\Phi_{m-1}(x,\eta)=\psi_{m-1}(x)-\eta,\quad D(x)=\|L_gV(x)\|+\|L_gL_f^{m-1}h(x)\|. \tag{14}$$

Note that the structure of the DETM (12) is similar to the DETM from [15]. However, while [15] focuses solely on event-triggered stability, this paper addresses both event-triggered safety and stability for nonlinear systems. Additionally, it is worth pointing out that for the event-triggered safety and stability of the system (1), it is not necessary for $\beta_h\alpha_m(\psi_{m-1}(x))+M\gamma(\Phi_{m-1}(x,\eta),t)-LD(x)\|e\|$ to always be non-negative based on the DETM (12). In fact, when $\eta_0\geq 0$, $\eta(t)$ can be ensured to remain non-negative for all $t\geq t_0$ by appropriately triggering events. Therefore, the term $\eta(t)$ in the DETM (12) can introduce additional stringency to the triggering condition, potentially causing delays in triggering events.

Moreover, the presence of $\Phi_{m-1}(x(t),\eta(t))\geq 0$ for all $t\geq t_0$ implies that the term $M\gamma(\Phi_{m-1}(x,\eta),t)$ in the DETM (12) can also introduce additional stringency to the triggering condition, potentially causing delays in triggering events. In other words, $\eta(t)$ and $M\gamma(\Phi_{m-1}(x,\eta),t)$ can lengthen the intervals between triggers. This effect becomes particularly noticeable when the Lipschitz constant L in Assumption 2.3 is conservatively set to a large value. However, it is essential to recognize that the value of $M\gamma(\Phi_{m-1}(x,\eta),t)$ involves a trade-off between triggering intervals and convergence speed.

Remark 3.1: A comparison between the proposed event-triggered mechanism (12) and existing ones is as follows. The event-triggered mechanisms in [25], [26] consist of three or seven triggering conditions, whereas (12) involves only one triggering condition, making its structure simpler. Moreover, the mechanisms in [25], [26] rely on computing state and error bounds, which can lead to excessive computations. In contrast, (12) eliminates the need for such computations, resulting in higher computational efficiency.

To illustrate the positive value feature of the dynamic variable $\eta(t)$ defined in (13), we first provide a preliminary lemma.

Lemma 3.1: For the controller (6) with the DETM (12) and (13), the dynamic variable $\eta(t)$ satisfies $\eta(t)\geq 0$, $\forall t\geq t_0$.

Proof: For all $t\geq t_0$, the DETM (12) ensures

$$\eta(t)+\theta_h\big(\beta_h\alpha_m(\psi_{m-1}(x(t)))+M\gamma\big(\Phi_{m-1}(x(t),\eta(t)),t\big)-LD(x(t))\|e(t^-)\|\big)\geq 0,$$

because an event is triggered before the left-hand side of the inequality becomes negative. Also, the definition of $e(t)$ in (11) gives $\|e(t)\|\leq\|e(t^-)\|$. Therefore, it is easy to verify that

$$\beta_h\alpha_m(\psi_{m-1}(x(t)))+M\gamma\big(\Phi_{m-1}(x(t),\eta(t)),t\big)-LD(x(t))\|e(t)\|\geq-\frac{1}{\theta_h}\eta(t). \tag{15}$$

It is deduced from (13) and (15) that

$$\dot\eta(t)\geq-\delta_h\eta(t)-\frac{1}{\theta_h}\eta(t),\ \eta(t_0)=\eta_0>0.$$

By means of the comparison lemma [34], one obtains

$$\eta(t)\geq\eta_0e^{-(\delta_h+\frac{1}{\theta_h})(t-t_0)}\geq 0,\ t\geq t_0, \tag{16}$$

which completes the proof. ■

B. Forward-Invariance and Zeno-Free

The first main theorem, presented below, demonstrates the event-triggered emulation of the safety-critical controller using the proposed DETM, thereby achieving properties P1 and P3.

Theorem 3.1: Consider the system (1) with the controller (6) and the DETM (12) and (13), where the control function k is given in Theorem 2.1 for a compact forward-invariant set

$\mathscr{S}$ with $0 \in \text{Int}\mathscr{S}$ and $0 < \eta_0 \le \psi_{m-1}(x_0)$. Under Assumptions 2.1, 2.2, and 2.3, if the two positive constants δ_h and β_h are chosen, such that

$$\frac{\delta_h}{1+\beta_h} \ge L_1,\ \overline{\alpha}\big(\alpha_v^{-1}(\beta_h L_2)\big) + \frac{\beta_h L_2}{\delta_h} < \min_{x \notin \text{Int}\mathscr{S}} V(x), \quad (17)$$

where L_1 and L_2 are given in (10) with $\mathscr{D} = \mathscr{S}$, and V, $\overline{\alpha}$, and α_v in (8), then properties P1 and P3 are achieved.

Proof: The two properties are proved in two separate steps below.

Proof of P1: First of all, the time derivative of $\Phi_{m-1}(x,\eta)$ defined in (14) satisfies, for $x \in \mathscr{S}$ and $\eta \in [0, \psi_{m-1}(x)]$,

$$\begin{aligned}\dot{\Phi}_{m-1}(x,\eta) =& \dot{\psi}_{m-1}(x) - \dot{\eta}\\ =& L_f^m h(x) + L_g L_f^{m-1} h(x) k(x) + O_{m-1}(x)\\ &+ L_g L_f^{m-1} h(x)\big[k(x+e) - k(x)\big] - \dot{\eta}\\ \ge& -\alpha_m\big(\psi_{m-1}(x)\big) - L\|L_g L_f^{m-1} h(x)\|\|e(t)\| - \dot{\eta}\\ \ge& -\alpha_m\big(\psi_{m-1}(x)\big) - LD(x)\|e(t)\| - \dot{\eta}\\ \ge& \delta_h\eta - (1+\beta_h)\alpha_m(\psi_{m-1}(x)) - M\gamma(\Phi_{m-1}(x,\eta),t).\end{aligned} \quad (18)$$

Using Assumption 2.1 and (10) with $L_1 \le \frac{\delta_h}{1+\beta_h}$ and the fact $\eta(t) \ge 0$ by Lemma 3.1, one has

$$\delta_h\eta - (1+\beta_h)\alpha_m(\psi_{m-1}(x)) \ge -(1+\beta_h)\alpha_m(\psi_{m-1}(x) - \eta).$$

Substituting this into (18) gives

$$\dot{\Phi}_{m-1}(x,\eta) \ge -(1+\beta_h)\alpha_m(\Phi_{m-1}(x,\eta)) - M\gamma(\Phi_{m-1}(x,\eta),t). \quad (19)$$

Next, by the definition of $\gamma(\Phi_{m-1}(x,\eta),t)$, consider the following two cases: i) If $\Phi_{m-1}(x,\eta) < 0$, then $\gamma(\Phi_{m-1}(x,\eta),t) \le 0$. Thus, (19) implies

$$\dot{\Phi}_{m-1}(x,\eta) \ge -(1+\beta_h)\alpha_m(\Phi_{m-1}(x,\eta)).$$

ii) If $\Phi_{m-1}(x,\eta) \ge 0$, then (19) yields

$$\dot{\Phi}_{m-1}(x,\eta) \ge -(1+\beta_h)\alpha_m(\Phi_{m-1}(x,\eta)) - M\gamma(\Phi_{m-1}(x,\eta),t_0).$$

These two cases together imply

$$\dot{\Phi}_{m-1}(x,\eta) \ge -\alpha_h(\Phi_{m-1}(x,\eta)), \quad (20)$$

for an extended class $\mathscr{K}_\infty$ function α_h defined as

$$\alpha_h(s) = \begin{cases}(1+\beta_h)\alpha_m(s), & s < 0,\\ (1+\beta_h)\alpha_m(s) + M\gamma(s,t_0), & s \ge 0.\end{cases}$$

Thus, if $\Phi_{m-1}(x_0,\eta_0) \ge 0$, then $\Phi_{m-1}(x(t),\eta(t)) \ge 0$ for all $t \ge t_0$. Therefore, according to $\Phi_{m-1}(x,\eta) = \psi_{m-1}(x) - \eta$ and (20) with $0 < \eta_0 \le \psi_{m-1}(x_0)$, one has

$$\psi_{m-1}(x(t)) \ge \eta(t) \ge 0,\ \forall t \ge t_0. \quad (21)$$

As a consequence, by (21) and the proof of Lemma 1 in [11], if $x_0 \in \mathscr{S}$ and $0 < \eta_0 \le \psi_{m-1}(x_0)$, then the solution $x(t)$ of the closed-loop system satisfies $x(t) \in \mathscr{S}$ for all $t \ge t_0$, which exhibits P1.

Proof of P3: We use the following candidate Lyapunov function $W : \mathbb{R}^n \times \mathbb{R}_{\ge 0} \to \mathbb{R}_{\ge 0}$ for the closed-loop system,

$$W(x,\eta) = V(x) + \eta. \quad (22)$$

Using Assumption 2.2 and the fact $\eta(t) \ge 0$ by Lemma 3.1, one has $W(x,\eta) \ge V(x) \ge 0$ and $W(x,\eta)$ is radially unbounded. Using Assumptions 2.2 and 2.3 gives

$$\begin{aligned}\dot{W} =& \dot{V}(x) + \dot{\eta}\\ =& L_f V(x) + L_g V(x) k(x+e) + \dot{\eta}\\ =& L_f V(x) + L_g V(x) k(x) + L_g V(x)\big[k(x+e) - k(x)\big] + \dot{\eta}\\ \le& -\alpha_v(\|x\|) + L\|L_g V(x)\|\|e(t)\| + \dot{\eta}\\ \le& -\alpha_v(\|x\|) + LD(x)\|e(t)\| + \dot{\eta}\\ \le& -\alpha_v(\|x\|) - \delta_h\eta + \beta_h\alpha_m(\psi_{m-1}(x)) + M\gamma(\Phi_{m-1},t).\end{aligned} \quad (23)$$

On the compact set $x(t) \in \mathscr{S}$, with (10) and the condition (21), the terms $\Phi_{m-1}(x(t),\eta(t))$ and $\alpha_m(\psi_{m-1}(x(t)))$ are bounded by L_2, for all $t \ge t_0$. Hence, by (23), one has

$$\dot{W} \le -\alpha_v(\|x\|) - \delta_h\eta + \beta_h L_2 + M\gamma(L_2,t). \quad (24)$$

Define

$$\Omega(t) = \Big\{(x,\eta) \in \mathbb{R}^n \times \mathbb{R}_{\ge 0} \mid \alpha_v(\|x\|) + \delta_h\eta \le \beta_h L_2 + M\gamma(L_2,t)\Big\}. \quad (25)$$

By (24) and (25), all the states of the closed-loop system converge to $\Omega(t)$. Since $M\gamma(L_2,t)$ goes to 0 as $t \to +\infty$, the convergence $\Omega(t) \to \Omega_\infty$ holds for

$$\Omega_\infty = \Big\{(x,\eta) \in \mathbb{R}^n \times \mathbb{R}_{\ge 0} \mid \alpha_v(\|x\|) + \delta_h\eta \le \beta_h L_2\Big\}. \quad (26)$$

In what follows, we will prove two claims.

Claim i: There exists a constant $\varepsilon > 0$ and hence a compact set

$$\overline{\Omega} = \{(x,\eta) \in \mathbb{R}^n \times \mathbb{R}_{\ge 0} \mid W(x,\eta) \le \varepsilon\},$$

such that $\Omega_\infty \subset \overline{\Omega}$ and $\psi_{min} = \min_{(x,\eta)\in\overline{\Omega}} \psi_{m-1}(x) > 0$.

To prove this claim, we define

$$\overline{W} = \min_{x \notin \text{Int}\mathscr{S}} V(x),\ \underline{W} = \overline{\alpha}\big(\alpha_v^{-1}(\beta_h L_2)\big) + \frac{\beta_h L_2}{\delta_h}, \quad (27)$$

that satisfies $\underline{W} < \overline{W}$ by (17). It is noted that $\overline{W} > 0$ holds as $0 \in \text{Int}\mathscr{S}$. Thus, a constant $\varepsilon \in (\underline{W}, \overline{W})$ exists.

For any $(x,\eta) \in \Omega_\infty$, one has $\|x\| \le \alpha_v^{-1}(\beta_h L_2)$ and $\eta \le \frac{\beta_h L_2}{\delta_h}$ by (26), and hence

$$W(x,\eta) = V(x) + \eta \le \overline{\alpha}(\|x\|) + \eta \le \underline{W} < \varepsilon.$$

It concludes $\Omega_\infty \subset \overline{\Omega}$ according to the definition of $\overline{\Omega}$.

For any $(x,\eta) \in (\mathbb{R}^n \setminus \text{Int}\mathscr{S}) \times \mathbb{R}_{\ge 0}$, that is, $x \notin \text{Int}\mathscr{S}$ and $\eta \in \mathbb{R}_{\ge 0}$, one has $W(x,\eta) = V(x) + \eta \ge \overline{W}$. But for any $(x,\eta) \in \overline{\Omega}$, one has $W(x,\eta) \le \varepsilon < \overline{W}$. Therefore, $\overline{\Omega}$ and $(\mathbb{R}^n \setminus \text{Int}\mathscr{S}) \times \mathbb{R}_{\ge 0}$ do not overlap, meaning that $\overline{\Omega} \subset \text{Int}\mathscr{S} \times \mathbb{R}_{\ge 0}$. Because of the facts that $\psi_{m-1}(x) > 0$ for $x \in \overline{\Omega} \subset \text{Int}\mathscr{S}$ and $\overline{\Omega}$ is a compact set, $\psi_{min} > 0$ is proved. Therefore, Claim i holds.

Claim ii: The state trajectory of the closed-loop system enters $\overline{\Omega}$ within a finite time T and stays in the set afterward.

Due to $\Omega_\infty \subset \overline{\Omega}$ in Claim i and the fact $\Omega(t)$ decreases to Ω_∞ as $t \to \infty$, we can always find a time $t^* > t' \ge t_0$ such that $\Omega(t^*) \subset \Omega(t') \subset \overline{\Omega}$. Define a constant $\ell = M\gamma(L_2,t') - M\gamma(L_2,t^*) > 0$.

Next, we analyze the system behavior for $t \geq t^*$. If $W(x,\eta) \geq \varepsilon$, then $(x,\eta) \notin \text{Int}\overline{\Omega}$ and hence $(x,\eta) \notin \text{Int}\Omega(t')$. As a result, one has $\alpha_v(\|x\|) + \delta_h \eta \geq \beta_h L_2 + M\gamma(L_2, t')$. Further calculation following (24) gives

$$\begin{aligned}\dot{W}(x,\eta) \leq & -\alpha_v(\|x\|) - \delta_h \eta + \beta_h L_2 + M\gamma(L_2, t^*) \\ = & -\alpha_v(\|x\|) - \delta_h \eta + \beta_h L_2 + M\gamma(L_2, t') - \ell \\ \leq & -\ell. \end{aligned} \tag{28}$$

If a state trajectory of the closed-loop system does not enter $\overline{\Omega}$ within a finite time T, then $(x(t), \eta(t)) \notin \overline{\Omega}$ and hence $W(x(t), \eta(t)) > \varepsilon$, for all $t \geq t^*$. By (28), one has

$$\begin{aligned} W(x(t), \eta(t)) \leq & W(x(t^*), \eta(t^*)) - \ell(t - t^*) \\ = & V(x(t^*)) + \eta(t^*) - \ell(t - t^*). \end{aligned} \tag{29}$$

Note that $x(t) \in \mathscr{S}$ and $\eta(t) \leq \psi_{m-1}(x(t)) \leq L_2$ for all $t \geq t_0$, and denote $\overline{V} = \max_{x \in \mathscr{S}} V(x)$. Further calculation following (29) gives

$$W(x(t), \eta(t)) \leq \overline{V} + L_2 - \ell(t - t^*) < \varepsilon, \tag{30}$$

for a sufficiently large t, which is a contradiction. Therefore, the state trajectory enters $\overline{\Omega}$ within a finite time T. Moreover, when a state trajectory is on the boundary of $\overline{\Omega}$, that is, $W(x,\eta) = \varepsilon$, it moves inwards due to (28). Therefore, the state trajectory stays in $\overline{\Omega}$. Claim (ii) is thus proved.

With the two claims in hand, we can continue the proof as follows. Consider any triggering instant t_{i+1}, $i \in \mathbb{I}$, at which the measurement error $e(t)$ is reset to zero by (11), i.e., $\|e(t_{i+1}^+)\| = 0$. But just before the triggering, the following inequality can be obtained from (12),

$$LD(x(t_{i+1}^-))\|e(t_{i+1}^-)\| \geq \frac{1}{\theta_h}\eta(t_{i+1}^-) + \beta_h \alpha_m(\psi_{m-1}(x(t_{i+1}^-))), \tag{31}$$

noting $M\gamma\big(\Phi_{m-1}(x(t_{i+1}^-), \eta(t_{i+1}^-)), t_{i+1}^-\big) \geq 0$.

Since $x(t) \in \mathscr{S}$ for all $t \geq t_0$, $D(x(t))$ and $\dot{x}(t)$ are bounded and denoted as $D(x) \leq \overline{D}$ and $\|\dot{x}(t)\| \leq L_3$ for two positive constants L_3 and $\overline{D}$. Thus, by (11), one has

$$\begin{aligned} LD(x)\|e(t)\| \leq & L\overline{D}\|e(t)\| = L\overline{D}\|x(t) - x(t_i)\| \\ \leq & L\overline{D}L_3(t - t_i), \forall t \in [t_i, t_{i+1}). \end{aligned} \tag{32}$$

Substituting (32) into (31) and noting (16) gives

$$\begin{aligned} t_{i+1} - t_i \geq & \frac{1}{L\overline{D}L_3}\Big(\frac{1}{\theta_h}\eta(t_{i+1}) + \beta_h \alpha_m(\psi_{m-1}(x(t_{i+1})))\Big) \\ \geq & \frac{1}{L\overline{D}L_3}\Big(\frac{\eta_0 e^{-(\delta_h + \frac{1}{\theta_h})(t_{i+1} - t_0)}}{\theta_h} + \beta_h \alpha_m(\psi_{m-1}(x(t_{i+1})))\Big). \end{aligned}$$

When $t_{i+1} < T$, one has $t_{i+1} - t_i \geq \Delta_1$ for

$$\Delta_1 = \frac{1}{L\overline{D}L_3}\Big(\frac{\eta_0 e^{-(\delta_h + \frac{1}{\theta_h})(T - t_0)}}{\theta_h}\Big) > 0.$$

When $t_{i+1} \geq T$, one has $(x(t_{i+1}), \eta(t_{i+1})) \in \overline{\Omega}$ by Claim ii and hence $\psi_{m-1}(x(t_{i+1})) \geq \psi_{min} > 0$ by Claim i. As a result, $t_{i+1} - t_i \geq \Delta_2$ for

$$\Delta_2 = \frac{1}{L\overline{D}L_3}\Big(\beta_h \alpha_m(\psi_{min})\Big) > 0.$$

From above, $t_{i+1} - t_i \geq \min\{\Delta_1, \Delta_2\} > 0$, $i \in \mathbb{I}$, which exhibits P3. ■

Remark 3.2: The assurance of property P2 is not provided by Theorem 3.1. However, this specific property will be subject to thorough investigation in the following section, where an improved event-triggered mechanism will be explored. Nonetheless, the theorem does establish a certain form of weak convergence for the system state. Indeed, it is observed in the proof that the system state converges to the set Ω_∞, as defined in (26). This set can be made arbitrarily small in proximity to the origin by making careful choices of the design parameters δ_h and β_h.

Remark 3.3: It is worth noting that a higher value of $M\gamma(\Phi_{m-1}(x,\eta), t)$ results in a greater right-hand side value in (24), which, in turn, leads to a slower convergence rate. In this design approach, the selection of $M\gamma(\Phi_{m-1}(x,\eta), t)$ is made with the intention of ensuring its convergence to zero as $t \to \infty$.

Remark 3.4: In Theorem 3.1, it is crucial to assume $0 \in \text{Int}\mathscr{S}$ for the existence of an MIET to exclude the Zeno phenomenon. Otherwise, if $0 \notin \text{Int}\mathscr{S}$, then $\overline{W} = 0$ according to its definition in (27). Consequently, $\varepsilon > 0$ satisfying $\varepsilon \in (\underline{W}, \overline{W})$ does not exist. Hence, the set $\overline{\Omega}$ relying on $\varepsilon > 0$ does not exist, and Claims i and ii no longer hold. More discussion about the exclusion of Zeno phenomenon is provided below. It is noted that $\dot{\Phi}_{m-1}(x(t), \eta(t))$ within $\mathscr{S} \times \mathbb{R}_{\geq 0}$ could be less than 0, implying that $\Phi_{m-1}(x(t), \eta(t))$ monotonically decreases over time. Additionally, as $\eta(t)$ may approach zero, so does $\psi_{m-1}(x(t))$. In other words, the system trajectory $x(t)$ may approach the boundary $\partial\mathscr{S}$. In Claims i and ii, the system trajectory enters the set $\overline{\Omega}$ that does not contain the boundary because $\overline{\Omega} \subset \text{Int}\mathscr{S} \times \mathbb{R}_{\geq 0}$. We have $\psi_{\min} = \min_{(x,\eta) \in \overline{\Omega}} \psi_{m-1}(x) > 0$. However, on the boundary $\partial\mathscr{S}$, $\psi_{\min} = \min_{x \in \partial\mathscr{S}} \psi_{m-1}(x)$, which is no longer a positive value. In the proof of Theorem 3.1, if T is infinite (a finite T does not exist), we do not have $\Delta_1 > 0$, and if T is finite, without a positive $\psi_{\min}$, we do not have $\Delta_2 > 0$, which results in failure to prove the exclusion of Zeno phenomenon.

To prevent the Zeno phenomenon in the case of $0 \notin \text{Int}\mathscr{S}$, we introduce a stronger barrier property than (5), which is given by

$$\sup_{u \in \mathbb{U}} \psi_m(x,u) \geq c, \ \ \forall x \in \mathscr{C}_1 \cap \cdots \cap \mathscr{C}_m, \tag{33}$$

where $c > 0$ is a predefined parameter. A corresponding HOCBF is defined. A new controller $k(x)$ based on this modified HOCBF can prevent the system trajectory $x(t)$ from approaching the boundary $\partial\mathscr{S}$. Specifically, the result (20) obtained in the proof of Theorem 3.1 becomes

$$\dot{\Phi}_{m-1}(x,\eta) \geq -\alpha_h(\Phi_{m-1}(x,\eta)) + c. \tag{34}$$

To replace the role of $\overline{\Omega}$ in the proof of Theorem 3.1, we define

$$\widetilde{\Omega} = \{(x,\eta) \in \mathbb{R}^n \times \mathbb{R}_{\geq 0} \mid \Phi_{m-1}(x,\eta) \geq \phi\}$$

for a parameter $\phi \in (0, \alpha_h^{-1}(c))$. If $\Phi_{m-1}(x,\eta) \leq \phi$, (34) implies

$$\dot{\Phi}_{m-1}(x,\eta) \geq -\alpha_h(\phi) + c > 0.$$

Since $\Phi_{m-1}(x(t_0),\eta(t_0)) \geq 0$, it takes a state trajectory up to a finite time $T = t_0 + \frac{\phi}{-\alpha_h(\phi)+c}$ to enter the set $\widetilde{\Omega}$ and stay in the set afterward. It is easy to verify that $\psi_{m-1}(x) = \Phi_{m-1}(x,\eta)+\eta \geq \phi$ in the set $\widetilde{\Omega}$. Therefore, we can still ensure that $\psi_{\min} = \min_{(x,\eta)\in\widetilde{\Omega}} \psi_{m-1}(x) \geq \phi > 0$. Then, we can use the same arguments in the proof of Theorem 3.1 to define two positive numbers Δ_1 and Δ_2 to characterize the MIET and hence prevent the Zeno phenomenon.

C. Asymptotic Convergence

The asymptotic convergence property P2 is further investigated in this subsection under an enhanced DETM, which is expressed as follows:

$$t_{i+1} = \inf_{t>t_i} \left\{ \begin{array}{l} t \in \mathbb{R}_{\geq 0} \Big| \eta(t) + \theta_h \Big(\beta_h \alpha_m(\psi_{m-1}(x(t))) \\ +M\gamma(\Phi_{m-1}(x(t),\eta(t)),t) - LD(x(t))\|e(t^-)\| \Big) \leq 0 \\ \text{or } \zeta(t) + \theta_v \Big(\beta_v \alpha_v(\|x(t)\|) \\ -L\|L_g V(x(t))\|\|e(t^-)\| \Big) \leq 0 \end{array} \right\}, \tag{35}$$

where η is the same dynamic variable satisfying (13), and ζ is an additional dynamic variable governed by

$$\dot{\zeta} = -\delta_v \zeta + \beta_v \alpha_v(\|x\|) - L\|L_g V(x)\|\|e\|, \ \zeta(t_0) = \zeta_0 \geq 0. \tag{36}$$

In the design, $\beta_v \in (0,1)$, θ_v, and δ_v are some positive parameters, and α_v and V are defined in (8). The additional triggering condition in (35) generally triggers more events to ensure the asymptotic convergence property P2, while it demands a stricter analysis of the Zeno phenomenon.

Remark 3.5: It is worth noting that the term $D(x)$ used in (35) and (13) can be substituted with its constituent part $\|L_g L_f^{m-1} h(x)\|$, considering that the other component, $\|L_g V(x)\|$, is already accounted for by the ζ dynamics. This substitution offers the advantage of postponing event triggers, thereby lengthening the intervals between triggers. This principle also holds true for the intermittent triggered mechanisms (45) and (46), which we will delve into later. Nevertheless, for the sake of theoretical proof, we will retain the term $D(x)$ in (35) and (13), allowing us to directly apply Theorem 3.1. Even with $D(x)$ replaced by $\|L_g L_f^{m-1} h(x)\|$, Theorem 3.1 remains applicable; however, some minor adjustments are necessary.

Remark 3.6: The result in Lemma 3.1 still holds. Using similar arguments, the dynamic variable $\zeta(t)$ also satisfies $\zeta(t) \geq 0$, $\forall t \geq t_0$.

The next theorem demonstrates the event-triggered emulation of the safety-critical controller using the enhanced DETM, achieving all three properties.

Theorem 3.2: Consider the system (1) with the controller (6) and the DETM (35), (13), and (36), where the control function k and the set $\mathscr{S}$ are given in Theorem 2.1 with $0 \in \text{Int}\mathscr{S}$ and $0 < \eta_0 \leq \psi_{m-1}(x_0)$. Under Assumptions 2.1, 2.2, and 2.3, if the two positive constants δ_h and β_h are chosen satisfying (17), then properties P1, P2, and P3 are achieved.

Proof: Compared to Theorem 3.1, we present the additional proof for P2. Following that, we provide modified proofs for P1 and P3, both tailored to the revised DETM.

Proof of P2: Consider the candidate Lyapunov function

$$W(x,\zeta) = V(x) + \zeta, \tag{37}$$

which is radially unbounded, using arguments similar to those for $W(x,\eta)$ in (22). By applying Assumptions 2.2 and 2.3, we obtain

$$\begin{aligned} \dot{W}(x,\zeta) &= \dot{V}(x) + \dot{\zeta} \\ &= L_f V(x) + L_g V(x) k(x+e) + \dot{\zeta} \\ &= L_f V(x) + L_g V(x) k(x) + L_g V(x) \big[k(x+e) - k(x)\big] + \dot{\zeta} \\ &\leq -\alpha_v(\|x\|) + L\|L_g V(x)\|\|e(t)\| + \dot{\zeta} \\ &\leq -\delta_v \zeta - (1-\beta_v)\alpha_v(\|x\|) \leq 0. \end{aligned} \tag{38}$$

Consequently, every trajectory of the closed-loop system asymptotically converges to the origin, and P2 is established.

Furthermore, by (38), for $\forall t \geq t_0$, $W(x,\zeta) \leq W(x_0,\zeta_0)$, which implies that all trajectories of the closed-loop system remain in a compact set with respect to initial states (x_0^T,ζ_0). In particular, we have $x(t) \in \mathscr{B}$ for a compact set $\mathscr{B} = \{x \in \mathbb{R}^n | V(x) \leq W(x_0,\zeta_0)\}$.

Proof of P1: The proof of P1 essentially follows the approach presented in Theorem 3.1. Given that the proof of P2 establishes that all trajectories of the closed-loop system remain within a compact set with respect to the initial states (x_0^T,ζ_0), the proof of P1 in Theorem 3.1 holds without explicitly assuming that $\mathscr{S}$ is a compact set. Specifically, the solution $x(t)$ satisfies $x(t) \in \mathscr{D}$, where $\mathscr{D}$ is a compact set such that $\mathscr{B} \cap \mathscr{S} \subset \mathscr{D}$. Moreover, this compact set $\mathscr{D}$ is used to determine the constants L_1 and L_2 in (10).

Proof of P3: It is observed that an event is triggered if either of the two conditions in (35) is satisfied. In Theorem 3.1, we have already established the existence of an MIET $\min\{\Delta_1,\Delta_2\}$ for events triggered by the first condition in (35). Now, we will demonstrate the existence of an MIET for the second condition in (35), which gives rise to property P3. The proof follows a similar approach to that used in [15], [17] and is elaborated below.

With $\zeta(t) \geq 0$ for all $t \geq t_0$, the second condition in (35) is satisfied only if

$$\beta_v \alpha_v(\|x(t)\|) - L\|L_g V(x(t))\|\|e(t^-)\| \leq 0. \tag{39}$$

By the same fact $\|L_g V(x)\| \leq D(x) \leq \overline{D}$ used in the proof of Theorem 3.1, we have

$$\beta_v \alpha_v(\|x(t)\|) - L\|L_g V(x(t))\|\|e(t^-)\| \geq \beta_v \alpha_v(\|x(t)\|) - L\overline{D}\|e(t^-)\|.$$

In other words, (39) implies $\beta_v \alpha_v(\|x(t)\|) \leq L\overline{D}\|e(t^-)\|$ or equivalently

$$\|x(t)\| \leq \alpha_v^{-1}\left(\frac{L\overline{D}}{\beta_v}\|e(t^-)\|\right). \tag{40}$$

Since $x(t) \in \mathscr{D}$ for a compact set $\mathscr{D}$, $e(t)$ is also in a compact set due to (11). Therefore, there exists a constant $P > 0$ such that

$$\alpha_v^{-1}\left(\frac{L\overline{D}}{\beta_v}\|e\|\right) \leq P\|e\|.$$

In conclusion, the second condition in (35) is satisfied only if $\|x(t)\| \le P\|e(t^-)\|$ is satisfied. Thus, it suffices to show that there is an MIET for the ETM

$$t_{i+1} = \inf_{t>t_i} \left\{ t \in \mathbb{R}_{\ge 0} \middle| \|x(t)\| \le P\|e(t^-)\| \right\}. \tag{41}$$

Since $f_c \triangleq f(x)+g(x)k(x)$ is locally Lipschitz with $f(0)=0$ and $k(0)=0$, $x(t)$ and $e(t)$ are in compact sets, there exists a constant $L_m>0$ for $f_c(x,e)=f(x)+g(x)u(x+e)$, such that

$$\|f_c(x,e)-f_c(x',e')\| \le L_m\|(x,e)-(x',e')\|,$$

which implies that

$$\begin{aligned}\|\dot e\| =& \|\dot x(t)\| = \|f(x)+g(x)u(x+e)\| \\ =& \|f_c(x,e)\| = \|f_c(x,e)-f_c(0,0)\| \le L_m\|x\|+L_m\|e\|.\end{aligned} \tag{42}$$

Therefore, the time derivative of $y=\frac{\|e\|}{\|x\|}$ satisfies

$$\dot y = \frac{d}{dt}\frac{\|e\|}{\|x\|} \le L_m(1+\frac{\|e\|}{\|x\|})^2 = L_m(1+y)^2. \tag{43}$$

It is noted that $\phi(t)=\frac{tL_m}{1-tL_m}$ is the analytical solution to the differential equation $\dot\phi = L_m(1+\phi)^2$ with $\phi(0)=0$. Let $\Delta_3 = \frac{1}{PL_m+L_m} > 0$ be the constant satisfying $\phi(\Delta_3)=P^{-1}$. By the comparison lemma [34], it takes $y=\frac{\|e\|}{\|x\|}$ more than Δ_3 to move from 0 or P^{-1} to trigger an event based on (41). That is, the inter-execution times are bounded by Δ_3, which characterizes an MIET for the second condition in (35). The proof is thus completed. ∎

Remark 3.7: The Lyapunov functions $W(x,\eta)$ and $W(x,\zeta)$ are utilized in the proofs of Theorems 3.1 and 3.2 to address the composite dynamics of x and η, and x and ζ, respectively. Each of these dynamics possesses an implicitly ISS property, and their combination ensures the stability of the closed-loop system. It should be noted that we do not assume ISS for the system $\dot x = f(x)+g(x)k(x+e)$ with e as the input, as in [15], [21]. Additionally, $\mathscr{D}=\mathscr{S}$ or $\mathscr{B}\cap\mathscr{S}\subset\mathscr{D}$ for a compact set $\mathscr{D}$ ensures that the state x remains bounded. This facilitates the existence of constants L, L_1, and L_2, and hence the calculation of the time derivative of $W(x,\eta)$.

IV. Intermittent Emulation

In this section, we extend the results developed in Section III to intermittent emulation of the safety-critical controller. This emulation involves the use of two types of triggering mechanisms: one to activate and another to deactivate the controller. Their designs are discussed below.

A. Triggering Control Deactivation

When the controller is active, with the intermittent emulation (7), the measurement error is slightly modified to

$$e(t) = x(t_i^{\rm on}) - x(t),\ \forall t \in [t_i^{\rm on}, t_i^{\rm off}),\ \text{for } i \in \mathbb{I}. \tag{44}$$

The error is utilized in designing the triggering mechanism for control deactivation. On the interval $\left[t_i^{\rm off}, t_{i+1}^{\rm on}\right)$ (when the controller is off), the measurement error is not required and, therefore, not necessarily defined.

The triggering mechanism for control deactivation is similar to that used in Theorem 3.2. The difference is that, once an event is triggered, the controller is immediately updated in Theorem 3.2, while in the current framework, the controller is turned off and will wait for another event to be turned on and updated again. The modified triggering mechanism, derived from (35), is given as follows:

$$t_i^{\rm off} = \inf_{t>t_i^{\rm on}} \left\{ \begin{array}{l} t \in \mathbb{R}_{\ge 0} \Big| \eta(t) + \theta_h\Big(\beta_h\alpha_m(\psi_{m-1}(x(t))) + \\ M\gamma(\Phi_{m-1}(x(t),\eta(t)),t) - LD(x(t))\|e(t^-)\|\Big) \le 0 \\ \text{or } \zeta(t) + \theta_v\Big(\beta_v\alpha_v(\|x(t)\|) - L\|L_gV(x(t))\|\|e(t^-)\|\Big) \le 0 \end{array} \right\}. \tag{45}$$

The only difference is that (35) determines t_{i+1}, but (45) determines $t_i^{\rm off}$. The two dynamics (13) and (36) governing η and ζ are accordingly changed to:

$$\begin{aligned}\dot\eta =& -\delta_h\eta + \beta_h\alpha_m\big(\psi_{m-1}(x)\big) + M\gamma\big(\Phi_{m-1}(x,\eta),t\big) \\ & - LD(x)\|e\|,\ \forall\, t \in \left[t_i^{\rm on}, t_i^{\rm off}\right), \\ & 0 < \eta(t_i^{\rm on}) \le \psi_{m-1}(x(t_i^{\rm on})),\end{aligned} \tag{46}$$

and

$$\begin{aligned}&\dot\zeta = -\delta_v\zeta + \beta_v\alpha_v(\|x\|) - L\|L_gV(x)\|\|e\|,\ \forall\, t \in \left[t_i^{\rm on}, t_i^{\rm off}\right), \\ &\dot\zeta = 0,\ \forall\, t \in \left[t_i^{\rm off}, t_{i+1}^{\rm on}\right),\ 0 \le \zeta_0 \le \beta_\zeta(\|x_0\|),\end{aligned} \tag{47}$$

for a class $\mathscr{K}_\infty$ function β_ζ.

B. Triggering Control Activation

We next discuss the conditions under which the controller is triggered back to activation. Without activating the controller, the system may lose stability, and the set $\mathscr{S}$ may no longer be forward invariant. Therefore, it is essential to trigger the controller back into activation to prevent this from happening. For this purpose, we leverage some performance-barrier-based trigger design ideas to specify two functions that restrict the tendency of the functions $W(x,\zeta)$ defined in (37) and $\psi_{m-1}(x)$ in (3). These two functions are defined as follows.

A performance specification function $S_v(t):\mathbb{R}_{\ge 0}\to\mathbb{R}_{\ge 0}$ is a piecewise continuously differentiable function that satisfies the properties:

(i) $S_v(t_i^{\rm off}) > W(x(t_i^{\rm off}),\zeta(t_i^{\rm off}))$, $i\in\mathbb{I}$,
(ii) $\lim_{t\to\infty} S_v(t) = 0$, and
(iii) it has an upper bound $S_{\max} \le W(x_0,\zeta_0)$.

A forward-invariant set constraint function $S_h(t):\mathbb{R}_{\ge 0}\to\mathbb{R}_{\ge 0}$ is a piecewise continuously differentiable function that satisfies $S_h(t_i^{\rm off}) < \psi_{m-1}(x(t_i^{\rm off}))$, $i\in\mathbb{I}$.

Remark 4.1: The values of the two functions $S_v(t)$ and $S_h(t)$ on $[t_i^{\rm off}, t_{i+1}^{\rm on})$ are important for triggering control activation, while the values on $[t_i^{\rm on}, t_i^{\rm off})$ (when the controller is on) are not useful. The specific design of the functions on $[t_i^{\rm off}, t_{i+1}^{\rm on})$ can be done at each time $t_i^{\rm off}$. For example, $S_v(t)$ can be chosen as $S_v\left(t_i^{\rm off}\right) = \left[W(x(t_i^{\rm on}),\zeta(t_i^{\rm on})) + W(x(t_i^{\rm off}),\zeta(t_i^{\rm off}))\right]/2$ and $\dot S_v = -\lambda_v S_v$ on $[t_i^{\rm off}, t_{i+1}^{\rm on})$ for a positive constant λ_v. Also, $S_h(t)$ can be chosen as a constant function, such as $S_h(t)=S_i$ on $[t_i^{\rm off}, t_{i+1}^{\rm on})$ for a positive constant $S_i < \psi_{m-1}(x(t_i^{\rm off}))$. It is

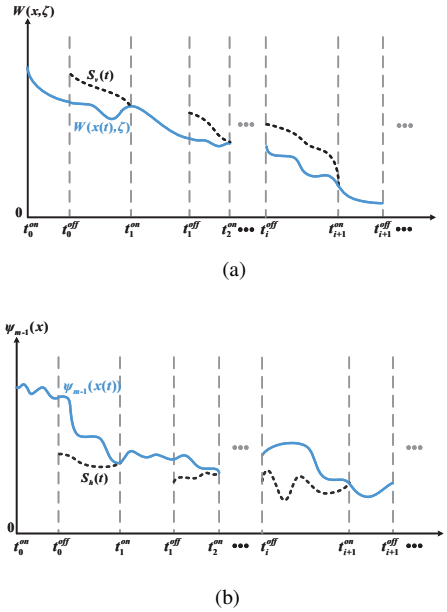

(a)

(b)

Fig. 1: Illustration of the triggering mechanisms for intermittent emulation.

worth noting that the property $S_{\max} \leq W(x_0, \zeta_0)$ ensures that the system performance is not worse than that at the initial time t_0.

Fig. 1 shows an overview of the intermittent control scheme. More specifically, $W(x,\zeta)$ is strictly decreasing and $\psi_{m-1}(x) \geq 0$ when the controller is on. It is expected that the system does not violate the performance specification and the forward-invariant set constraint, that is, $W(x(t),\zeta(t)) \leq S_v(t)$ and $\psi_{m-1}(x(t)) \geq S_h(t)$ are always guaranteed when the controller is off. In other words, when either of these two conditions is violated, the controller must be turned on. It motivates a triggering mechanism for control activation as follows:

$$t_{i+1}^{\text{on}} = \inf_{t > t_i^{\text{off}}} \Big\{ t \in \mathbb{R}_{\geq 0} \Big| W(x(t),\zeta(t)) \geq S_v(t^-) \text{ or } \psi_{m-1}(x(t)) \leq S_h(t^-) \Big\}. \tag{48}$$

C. Overall Analysis

The overall performance of the intermitted emulated system under the proposed control deactivation/activation triggering mechanisms is summarized in the following theorem.

Theorem 4.1: Consider the system (1) with the controller (6), the control deactivation triggering mechanism (45), (46), and (47), and the control activation triggering mechanism (48), where the control function k and the set $\mathscr{S}$ are given in Theorem 2.1 with $0 \in \text{Int}\mathscr{S}$, $0 < \eta_0 \leq \psi_{m-1}(x_0)$, and $0 \leq \zeta_0 \leq \beta_\zeta(\|x_0\|)$. Under Assumptions 2.1, 2.2, and 2.3, if the two positive constants δ_h and β_h are chosen satisfying (17), then properties P1, P2, and P3 are achieved.

Proof: The proof for the three properties is presented below in order.

Proof of P1: For any $t \in [t_i^{\text{on}}, t_i^{\text{off}})$, $i \in \mathbb{I}$, since $0 < \eta(t_i^{\text{on}}) \leq \psi_{m-1}(x(t_i^{\text{on}}))$ as set in (46), applying Theorem 3.2 ensures that $x(t) \in \mathscr{S}$. Due to the continuity of $x(t)$, we have $x(t_i^{\text{off}}) \in \mathscr{S}$. For any $t \in [t_i^{\text{off}}, t_{i+1}^{\text{on}})$, $i \in \mathbb{I}$, using the triggering condition (48), we obtain $\psi_{m-1}(x(t)) > S_h(t) \geq 0$. Then, given $x(t_i^{\text{off}}) \in \mathscr{S}$, the solution $x(t)$ of the closed-loop system satisfies $x(t) \in \mathscr{S}$. By combining the results over the two time intervals, we establish the proof of P1.

Proof of P2: For any $t \in [t_i^{\text{on}}, t_i^{\text{off}})$, $i \in \mathbb{I}$, the Lyapunov function $W(x(t),\zeta(t))$ defined in the proof of Theorem 3.2 monotonically decreases according to (38). Therefore, $W(x(t),\zeta(t)) \leq W(x(t_i^{\text{on}}),\zeta(t_i^{\text{on}})) \leq S_v(t_i^{\text{on}})$. As the value of S_v on the time interval $[t_i^{\text{on}}, t_i^{\text{off}})$ is irrelevant to the system behavior, it can be defined as $S_v(t) = S_v(t_i^{\text{on}})$ on this interval for the completeness of the proof here. As a result, we have $W(x(t),\zeta(t)) \leq S_v(t)$.

For any $t \in [t_i^{\text{off}}, t_{i+1}^{\text{on}})$, $i \in \mathbb{I}$, by using the property $S_v(t_i^{\text{off}}) > W(x(t_i^{\text{off}}),\zeta(t_i^{\text{off}}))$ and the triggering condition (48), we can ensure that $S_v(t) \geq W(x(t),\zeta(t))$.

By combining the results over the two time intervals, we have $0 \leq W(x(t),\zeta(t)) \leq S_v(t) \leq S_{\max} \leq W(x_0,\zeta_0)$, $\forall t \geq t_0$. Since the function $S_v(t)$ has the property $\lim_{t\to\infty} S_v(t) = 0$, we have $\lim_{t\to\infty} W(x(t),\zeta(t)) \leq \lim_{t\to\infty} S_v(t) = 0$. Thus, the state $x(t)$ has the convergence property $\lim_{t\to\infty} x(t) = 0$. Additionally, we have $x(t) \in \mathscr{D}$ for a compact set $\mathscr{D}$ as defined in the proof of Theorem 3.2.

Furthermore, since $S_{\max} \leq W(x_0,\zeta_0)$, we have

$$\begin{aligned} V(x(t)) &\leq W(x(t),\zeta(t)) \leq W(x_0,\zeta_0) \\ &\leq V(x_0) + \zeta_0 \leq V(x_0) + \beta_\zeta(\|x_0\|),\ \forall t \geq t_0. \end{aligned}$$

By Assumption 2.2, $\|x(t)\| \leq \underline{\alpha}^{-1}(\overline{\alpha}(\|x_0\|) + \beta_\zeta(\|x_0\|))$, $\forall t \geq t_0$, where the right-hand side of the inequality is a class $\mathscr{K}_\infty$ function of $\|x_0\|$. This verifies the stability of the equilibrium point $x = 0$. Together with the convergence property, the equilibrium point $x = 0$ of the closed-loop system is asymptotically stable. P2 is thus proved.

Proof of P3: To prevent Zeno behavior, we can employ the triggering design (45) and refer to Theorem 3.2 to establish an MIET, denoted as Δ, ensuring that $t_{i+1}^{\text{on}} - t_i^{\text{on}} > t_i^{\text{off}} - t_i^{\text{on}} \geq \Delta$. ■

Remark 4.2: The period during which the controller can remain inactive, known as the inactive dwell time as discussed in [22], directly impacts resource conservation. Consequently, the selection of functions $S_v(t)$ and $S_h(t)$ plays a critical role. Opting for relaxed choices of $S_v(t)$ and $S_h(t)$ allows more flexibility for the certificates $W(x,\zeta)$ and $\psi_{m-1}(x)$ to fluctuate before satisfying the trigger condition (48). This, in turn, enhances resource conservation but may result in slower convergence towards the origin.

V. Extension to Unknown Dynamics

We have investigated the digital emulation of the safety-critical controller $u = k(x)$ as outlined in Theorem 2.1. However, this theorem does not provide an explicit construction for the controller. In practical applications, this controller is typically derived by solving an optimization problem formulated as follows:

$$\begin{aligned} k(x) = &\underset{u}{\text{argmin}} \|u\|^2 \\ &\text{s.t.} \quad L_f V(x) + L_g V(x) u \leq -\alpha_v(\|x\|), \end{aligned}$$

$$\psi_m(x,u) \geq 0. \tag{49}$$

For ease of presentation, we define $G(x,u) = L_f V(x) + L_g V(x)u$. In event-triggered control, we only need to solve the optimization problem at discrete-time instances, such as t_i or t_i^{on}.

Clearly, the solvability of (49) hinges on having precise expressions for f and g. In this section, we aim to integrate an extended event-triggered intermittent control framework to address nonlinear systems in the presence of unknown dynamics. Specifically, while the exact forms of f and g in the system (1) may not be known, a nominal model can be represented as

$$\dot{x} = \tilde{f}(x) + \tilde{g}(x)u, \tag{50}$$

where $\tilde{f}(x) : \mathbb{R}^n \to \mathbb{R}^n$ and $\tilde{g}(x) : \mathbb{R}^n \to \mathbb{R}^{n\times q}$ are locally Lipschitz functions. Consequently, the system (1) can be reformulated as

$$\dot{x} = \tilde{f}(x) + \tilde{g}(x)u + b(x) + A(x)u, \tag{51}$$

where $b(x) = f(x) - \tilde{f}(x)$ and $A(x) = g(x) - \tilde{g}(x)$ denote the system uncertainties. A critical assumption concerning the uncertainties related to the HOCBF h in Theorem 2.1 is presented below. This assumption stipulates that the system (1) should maintain the same actuation capability as the nominal model (50), a standard assumption commonly employed in existing literature, such as [24], [35].

Assumption 5.1: The relative degree of h remains consistent between the nominal model (50) and the system (1); both possess a relative degree of m in the set $\mathscr{C}_1 \cap \cdots \cap \mathscr{C}_m$.

In the following discussion, we aim to elucidate how the terms $\psi_m(x,u)$ and $G(x,u)$, as utilized in (49), can be acquired from the nominal model (50). To accomplish this, we introduce a sequence of functions defined along the trajectory of the nominal model (50) as follows:

$$\begin{aligned}
\tilde{\psi}_0(x) &= h(x),\\
\tilde{\psi}_i(x) &= \dot{\tilde{\psi}}_{i-1}(x) + \alpha_i\big(\tilde{\psi}_{i-1}(x)\big), \quad i \in \{1,\ldots,m-1\},\\
\tilde{\psi}_m(x,u) &= \dot{\tilde{\psi}}_{m-1}(x) + \alpha_m\big(\tilde{\psi}_{m-1}(x)\big).
\end{aligned} \tag{52}$$

These functions bear a resemblance to those presented in (3) along the trajectory of the system (1). However, a notable distinction between them is explicitly delineated in the following proposition.

Proposition 5.1: If the system (1) and the nominal model (50) satisfy Assumption 5.1, then

$$\psi_i(x) = \tilde{\psi}_i(x) + \Delta_i(x),\ x \in \mathscr{C}_1 \cap \cdots \cap \mathscr{C}_m,\ i \in \{1,\ldots,m-1\}, \tag{53}$$

where $\psi_i(x)$ and $\tilde{\psi}_i(x)$ are defined in (3) and (52), respectively, and $\Delta_i(x)$ is a remainder term that is independent of the control input u.

Proof: The proof can be completed using a similar method as in [35], and is omitted here. In particular, $\Delta_i(x)$ can be explicitly expressed as follows:

$$\begin{aligned}
\Delta_1(x) &= \frac{\partial \tilde{\psi}_0(x)}{\partial x} b(x),\\
\Delta_i(x) &= \frac{\partial \tilde{\psi}_{i-1}(x)}{\partial x} b(x) + \alpha_i(\psi_{i-1}) - \alpha_i(\tilde{\psi}_{i-1})\\
&\quad + \frac{\partial \Delta_{i-1}(x)}{\partial x}\big[\tilde{f}(x) + b(x)\big],\ i = 2,\ldots,m-1.
\end{aligned}$$

These expressions are independent of the control input u. ■

Next, from (3) and (52), utilizing (53) with $i = m-1$, we obtain:

$$\begin{aligned}
\psi_m(x,u) =& \dot{\psi}_{m-1} + \alpha_m\big(\psi_{m-1}(x)\big)\\
=& \frac{\partial \tilde{\psi}_{m-1}(x)}{\partial x}\Big[\tilde{f}(x) + \tilde{g}(x)u\Big]\\
&+ \frac{\partial \tilde{\psi}_{m-1}(x)}{\partial x}\Big[b(x) + A(x)u\Big] + \alpha_m(\psi_{m-1})\\
&+ \frac{\partial \Delta_{m-1}(x)}{\partial x}\Big[\tilde{f}(x) + \tilde{g}(x)u + b(x) + A(x)u\Big],
\end{aligned}$$

and

$$\tilde{\psi}_m(x,u) = \frac{\partial \tilde{\psi}_{m-1}(x)}{\partial x}\big[\tilde{f}(x) + \tilde{g}(x)u\big] + \alpha_m(\tilde{\psi}_{m-1}).$$

Comparing these two expressions, we find

$$\psi_m(x,u) = \tilde{\psi}_m(x,u) + \Delta_m(x) + \Sigma_m(x)\,u, \tag{54}$$

where

$$\begin{aligned}
\Delta_m(x) =& \frac{\partial \tilde{\psi}_{m-1}(x)}{\partial x} b(x) + \frac{\partial \Delta_{m-1}(x)}{\partial x} \cdot \big[\tilde{f}(x) + b(x)\big]\\
&+ \alpha_m(\psi_{m-1}) - \alpha_m(\tilde{\psi}_{m-1}),\\
\Sigma_m(x) =& \frac{\partial \tilde{\psi}_{m-1}(x)}{\partial x} A(x) + \frac{\partial \Delta_{m-1}(x)}{\partial x} \cdot \big[\tilde{g}(x) + A(x)\big].
\end{aligned}$$

As a result, $\psi_m(x,u)$ can be computed based on the measurement $\tilde{\psi}_m(x,u)$ and estimates of the functions Δ_m and Σ_m.

To compute the term $G(x,u)$, we define the time derivative of $V(s)$ along the trajectory of the nominal model (50) as

$$\tilde{G}(x,u) = L_{\tilde{f}} V(x) + L_{\tilde{g}} V(x)u.$$

Then, we have:

$$\begin{aligned}
G(x,u) =& \frac{\partial V}{\partial x}\big[\tilde{f}(x) + \tilde{g}(x)u + b(x) + A(x)u\big]\\
=& \tilde{G}(x,u) + \Delta_v(x) + \Sigma_v(x)\,u,
\end{aligned} \tag{55}$$

where $\Delta_v(x) = \frac{\partial V}{\partial x} b(x)$ and $\Sigma_v(x) = \frac{\partial V}{\partial x} A(x)$. As a result, $G(x,u)$ can be computed based on the measurement $\tilde{G}(x,u)$ and estimates of the functions Δ_v and Σ_v.

Following the above development, we can apply a learning-based method to estimate the uncertainty functions Δ_m, Σ_m, Δ_v, and Σ_v, such as a neural network via supervised regression [36], [24]. We may conduct experiments to collect data by using a nominal state-feedback controller and learn functions that approximate the aforementioned functions. In particular, the terms $\psi_m(x,u)$ and $G(x,u)$ in (54) and (55) can be estimated as follows:

$$\begin{aligned}
\psi_{m,\theta}(x,u) &= \tilde{\psi}_m(x,u) + \alpha_\theta^h(x) + \beta_\theta^h(x)\,u,\\
G_\theta(x,u) &= \tilde{G}(x,u) + \alpha_\theta^V(x) + \beta_\theta^V(x)\,u,
\end{aligned}$$

where $\alpha_\theta^h(x)$, $\beta_\theta^h(x)$, $\alpha_\theta^V(x)$, and $\beta_\theta^V(x)$ represent the learning policies of neural network with parameters $\theta \in \mathbb{R}^N$. The goal of learning is to find θ to minimize the following loss functions

$$l_{\psi_m,\theta} = \big\|\psi_{m,\theta}(x,u) - \psi_m(x,u)\big\|^2,\ l_{G,\theta} = \|G_\theta(x,u) - G(x,u)\|^2.$$

With successful learning of the terms $\psi_m(x,u)$ and $G(x,u)$ by $\psi_{m,\theta}(x,u)$ and $G_\theta(x,u)$, the optimization problem (49) can be implemented as

$$\begin{aligned} k(x) =& \underset{u,\varepsilon}{\operatorname{argmin}} \|u\|^2 + p\varepsilon^2 \\ &\text{s.t. } G_\theta(x,u) \le -\alpha_v(\|x\|) + \varepsilon, \\ &\psi_{m,\theta}(x,u) \ge 0. \end{aligned} \tag{56}$$

Remark 5.1: The first constraint in the optimization problem (49) corresponds to (8) in Assumption 2.2. If this assumption does not hold, then the online optimization for (49) does not lead to the desired equilibrium point [37]. In such a case, the optimization problem can be relaxed to (56). The optimization problem (56) introduces a slack variable $\varepsilon \ge 0$ and a penalty factor $p > 0$ to relax the constraint (8) associated with the CLF. Including the slack variable enhances the solvability of the optimization problem and allows prioritization between forward invariance and convergence when these objectives conflict. However, the introduction of the slack variable means that the CLF condition specified in Assumption 2.2 is no longer satisfied. Instead, the inequality (8) is relaxed to:

$$L_f V(x) + L_g V(x) k(x) \le -\alpha_v\big(\|x\|\big) + \varepsilon.$$

It implicitly implies that the closed-loop system with $u = k(x)$ is ISS when ε is viewed as an input. When it is difficult to find a single controller satisfying both Assumptions 2.1 and 2.2 simultaneously, this relaxation makes the design of the controller more feasible. Consequently, under this relaxed condition, the closed-loop system achieves uniformly ultimately bounded stability rather than asymptotic stability due to the residual constant ε.

VI. Illustrative Examples

In this section, two examples are presented to illustrate the effectiveness of the proposed emulation methods. In the first example, we consider the event-triggered intermittent control for a known system with a third-order HOCBF. In the second example, we consider an adaptive cruise control example with unknown dynamics, and a learning-based method is applied.

A. An Academic Example

Consider a system of the form

$$\begin{aligned} \dot{x}_1 &= x_2, \\ \dot{x}_2 &= x_3, \\ \dot{x}_3 &= \sin(x_1) + u. \end{aligned} \tag{57}$$

We aim to design an event-triggered intermittent safety-critical controller for the system (57), where $\mathscr{C}_1 = \{x \in \mathbb{R}^3 : h(x) \ge 0\}$ with $x(t) = [x_1(t), x_2(t), x_3(t)]^T$ and $h(x) = 5 - x_1$.

The relative degree of h for the system (57) is $m = 3$. The functions in (3) can be explicitly calculated as

$$\begin{aligned} \psi_0(x) =& 5 - x_1, \\ \psi_1(x) =& -5x_1 - x_2 + 25, \\ \psi_2(x) =& -25x_1 - 10x_2 - x_3 + 125, \\ \psi_3(x,u) =& -125x_1 - 75x_2 - 15x_3 - \sin(x_1) + 625 - u, \end{aligned} \tag{58}$$

where $\alpha_1(\psi_0) = 5\psi_0$, $\alpha_2(\psi_1) = 5\psi_1$ and $\alpha_3(\psi_2) = 5\psi_2$ are used. We can construct the candidate Lyapunov function as follows:

$$V(x) = x_1^2 + (x_1 + x_2)^2 + (x_1 + 2x_2 + x_3)^2, \tag{59}$$

which satisfies $0.1\|x\|^2 \le V(x) \le 8\|x\|^2$. The time derivative of $V(x)$ along the system (57) satisfies

$$\begin{aligned} G(x,u) =& 2x_1x_2 + 2(x_1 + x_2)(x_2 + x_3) \\ &+ 2(x_1 + 2x_2 + x_3)[x_2 + 2x_3 + \sin(x_1) + u]. \end{aligned} \tag{60}$$

We simply take $\alpha_v(\|x\|)$ as $5V(x)$. Then, the safety-critical controller $u = k(x)$ is determined by solving the optimization problem (49) with $\psi_3(x,u)$, $V(x)$ and $G(x,u)$ in (58)-(60), that is,

$$\begin{aligned} k(x) =& \underset{u}{\operatorname{argmin}} \|u\|^2 \\ &\text{s.t. } G(x,u) \le -\alpha_v(\|x\|), \\ &\psi_3(x,u) \ge 0. \end{aligned} \tag{61}$$

It is difficult to theoretically verify Assumptions 2.1 and 2.2 simultaneously. However, the existence of an input u in the state space is numerically illustrated by the scatter diagram in Fig. 2. Each scatter point represents a state x for which $u = k(x)$ exists and satisfies the constraints in (61), corresponding to Assumptions 2.1 and 2.2.

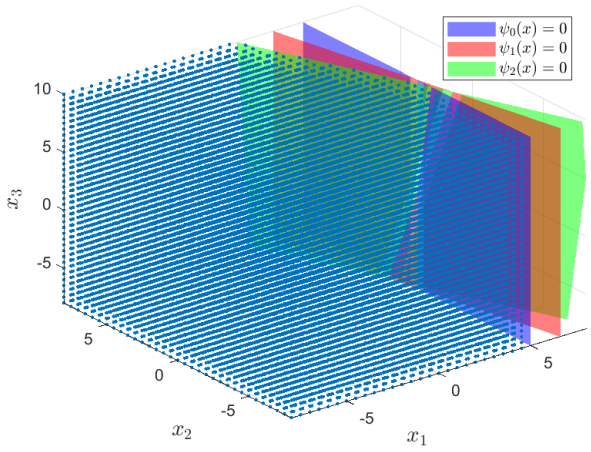

Fig. 2: Illustration of a subset of the state space where u exists.

This controller is implemented as (7) under the control deactivation triggering mechanism (45) and the control activation triggering mechanism (48) with

$$\begin{aligned} \dot{\eta} =& -\delta_h \eta + \beta_h \alpha_3\big(\psi_2(x)\big) + M\gamma\big(\Phi_2(x,\eta),t\big) \\ &- L\|L_g L_f^2 h(x)\|\|e\|, \ \eta(t_i^{\text{on}}) = 0.8\psi_2(x(t_i^{\text{on}})), \ \forall\, t \in \big[t_i^{\text{on}}, t_i^{\text{off}}\big), \\ \dot{\zeta} =& -\delta_v \zeta + \beta_v \alpha_v(\|x\|) - L\|L_g V(x)\|\|e\|, \ \forall\, t \in \big[t_i^{\text{on}}, t_i^{\text{off}}\big), \\ \dot{\zeta} =& 0, \ \forall\, t \in \big[t_i^{\text{off}}, t_{i+1}^{\text{on}}\big), \\ \zeta_0 =& 3, \end{aligned}$$

where $\Phi_2(x,\eta) = \psi_2(x) - \eta$, $L_g L_f^2 h = -1$ and $L_g V = 2x_1 + 4x_2 + 2x_3$. The parameters in the triggering mechanisms and the dynamic variables are given as follows: $\theta_h = \theta_v =$

This article has been accepted for publication in IEEE Transactions on Automatic Control. This is the author's version which has not been fully edited and content may change prior to final publication. Citation information: DOI 10.1109/TAC.2025.3574088

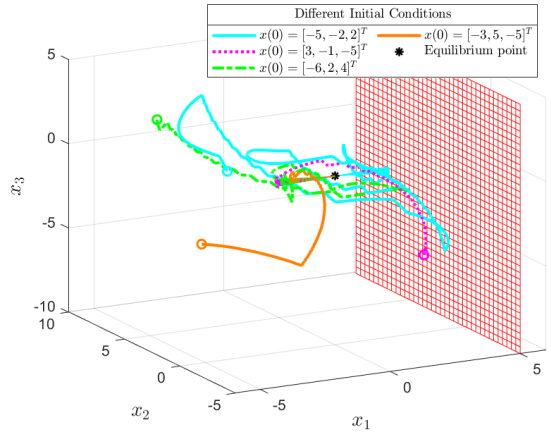

Fig. 3: State trajectories of the closed-loop system with different initial conditions are ensured within the safe region bounded the red grid lines.

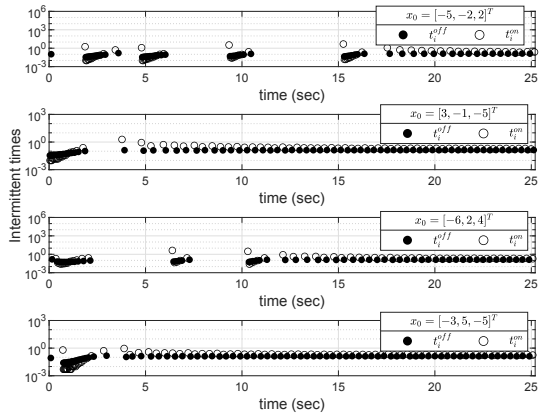

Fig. 4: Profile of intermittent times t_i^{on} and t_i^{off} for $i \in \mathbb{I}$ with different initial conditions.

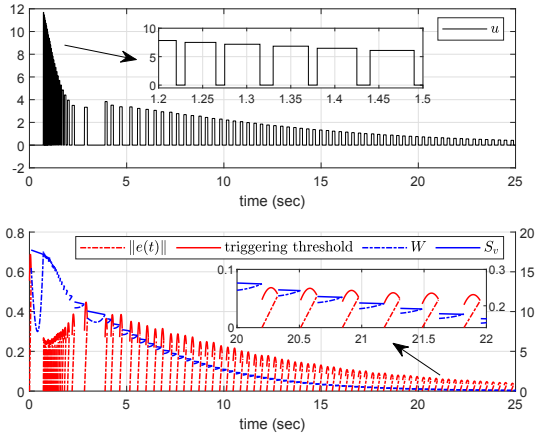

Fig. 5: Top: Evolution of the control signal $u(t)$; Bottom: Profile of $\|e(t)\|$, the triggering threshold, $W(x(t),\zeta(t))$, and $S_v(t)$ used in the triggering mechanisms.

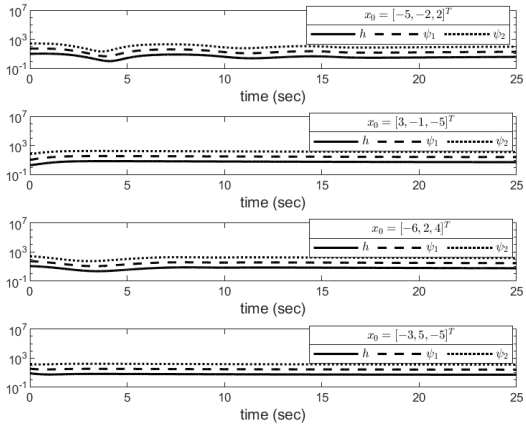

Fig. 6: Profile of $h(x)$, $\psi_1(x)$ and $\psi_2(x)$ with different initial conditions.

0.05, $\beta_h = 0.01$, $\beta_v = 0.6$, $M = 100$, $\delta_h = \delta_v = 1.01$, $L = 50$, and $\gamma(\Phi_2,t) = \Phi_2 e^{-5t}$. The functions $S_v(t)$ and $S_h(t)$ are specified as

$$S_v(t_i^{\text{off}}) = \big[W(x(t_i^{\text{on}}),\zeta(t_i^{\text{on}})) + W(x(t_i^{\text{off}}),\zeta(t_i^{\text{off}}))\big]/2,$$
$$\dot{S}_v = -0.05 S_v,\ \forall t \in [t_i^{\text{off}}, t_{i+1}^{\text{on}}),$$
$$S_h(t) = 0.5\psi_2(x(t_i^{\text{off}})),\ \forall t \in [t_i^{\text{off}}, t_{i+1}^{\text{on}}).$$

The effectiveness of the design is theoretically guaranteed by Theorem 4.1 and further demonstrated by numerical simulation. In the simulation, we examine the system behaviors under four different initial conditions: $[-5,-2,2]^T$, $[3,-1,-5]^T$, $[-6,2,4]^T$ and $[-3,5,-5]^T$. It is observed in Fig. 3 that the trajectories $x(t)$ always stay in the safe set $\mathscr{S}$ graphically represented by the region bounded with the one wall at $x_1 = 5$. The convergence to the equilibrium point at the origin is also observed. The time intervals between controller activations, also known as the intermittent times, are plotted in Fig. 4. This is consistent with the conclusion regarding the exclusion of the Zeno phenomenon.

The evolution of the controller $u(t)$ is plotted in the top graph of Fig. 5, which is piecewise constants, and the updates are determined by events. The graph also demonstrates that $u = k(x)$ satisfying both Assumptions 2.1 and 2.2 can be obtained. The signals for triggering events are plotted in the bottom graph. In particular, the measurement error $\|e(t)\|$ and the triggering threshold (the value $\|e(t)\|$ reaches to trigger an event according to (45)) are plotted in red, while the Lyapunov function $W(x(t),\zeta(t))$ and the performance specification function $S_v(t)$ are in blue. It is observed that $W(x(t),\zeta(t))$ converges to zero as $t \to \infty$. Also, when the controller is off, the forward-invariant set constraint function $S_h(t)$ is not activated and therefore it is not shown. Only the case with $x_0 = [-3,5,-5]^T$ is plotted here as the profiles with other initial values are similar. Finally, Fig. 6 demonstrates that $h(x)$, $\psi_1(x)$, and $\psi_2(x)$ are consistently positive, indicating the safety of the system (57) with respect to $\mathscr{C}_1 \cap \mathscr{C}_2 \cap \mathscr{C}_3$.

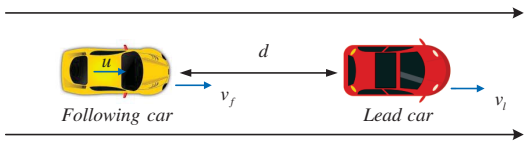

Fig. 7: Schematic diagram of adaptive cruise control.

B. Adaptive Cruise Control

In this example, we aim to verify the effectiveness of the proposed event-triggered control method in the adaptive cruise control (ACC) problem [11], [38], with a learning algorithm for unknown dynamics. The dynamics of the ACC system can be described as:

$$\underbrace{\begin{bmatrix} \dot{v}_l \\ \dot{v}_f \\ \dot{d} \end{bmatrix}}_{\dot{x}} = \underbrace{\begin{bmatrix} a_l \\ -F_r/m \\ v_l - v_f \end{bmatrix}}_{f(x)} + \underbrace{\begin{bmatrix} 0 \\ 1/m \\ 0 \end{bmatrix}}_{g(x)} u, \tag{62}$$

where v_l $[m/s]$ and v_f $[m/s]$ are the velocities of the lead car and the following car, respectively, and d $[m]$ is the distance between the lead and following cars, as depicted in Fig. 7. Also, $F_r = f_0\text{sgn}(v_f) + f_1 v_f + f_2 v_f^2$ $[N]$ is the aerodynamic drag, m $[kg]$ is the mass of the following car, a_l $[m/s^2]$ is the acceleration of the lead car, $\delta > 0$ $[m]$ is the length of the two vehicles, and v_d $[m/s]$ is a desired speed of the following car. The model uncertainty in this example is introduced by the mass and the aerodynamic drag. The parameters used in the simulation are listed in Table I (refer to [38]).

TABLE I: Parameters in adaptive cruise control.

Variable	Value	Unit
m	1650	kg
g	9.81	m/s^2
a_l	0	m/s^2
v_d	22	m/s
f_0	0.1	N
f_1	5	Ns/m
f_2	0.25	Ns^2/m^2
δ	10	m

The control objective for the following car is to maintain a safe following distance while cruising. Specifically, when sufficient headway is assured, the following car should reach a desired speed denoted as v_d. The safety constraint mandates that the following car maintains a safe distance from the lead car, expressed as $d \geq \delta$, where $\delta > 0$ represents the length of both vehicles. In this scenario, the equilibrium point lies outside the forward-invariant set, as explained in Remark 3.4.

For this control objective, we can define the safety constraint as $h(x) = d - \delta$, which possesses a relative degree of 2 for the system (62), where $\mathscr{C}_1 = \{x \in \mathbb{R}^3 : h(x) \geq 0\}$. The functions in (3) can be explicitly calculated as follows:

$$\begin{aligned} \psi_0(x) =& d - \delta, \\ \psi_1(x) =& v_l - v_f + d - \delta, \\ \psi_2(x,u) =& a_l + F_r/m - u/m + 2(v_l - v_f) + d - \delta, \end{aligned}$$

where $\alpha_1(\psi_0) = \psi_0$ and $\alpha_2(\psi_1) = \psi_1$ are utilized. As the only controlled state variable of the system (62) is the velocity of the following car v_f, we can employ a CLF $V(x) = \frac{1}{2}(v_f - v_d)^2$ to regulate v_f to v_d. The time derivative of $V(x)$ along the system (62) satisfies

$$G(x,u) = \left(v_f - v_d\right)\left(-F_r/m + u/m\right).$$

Since the mass and the aerodynamic drag of the following car are unknown, it is necessary to estimate $\psi_2(x,u)$ and $G(x,u)$ through supervised regression. To achieve this, any standard learning algorithm can be readily applied to learn the model uncertainty. In our approach, we employ a neural network framework with three hidden layers, each consisting of ten neurons. The training data for this learning process is generated by differentiation using a discrete time step of $t_s = 0.001$ $[sec]$. The final agent utilized is obtained after 3000 episodes of training.

The learned terms are denoted as $\psi_{2,\theta}(x,u)$ and $G_\theta(x,u)$. As a result, by selecting $\alpha_v(\|x\|) = 6V(x)$, the optimization problem (56) can be formulated. However, some modifications to (56) are necessary in this example, leading to the following formulation:

$$\begin{aligned} k(x(t_i)) =& \underset{u,\varepsilon}{\text{argmin}} \|u - F_{r,\theta}\|^2 + p\varepsilon^2 \\ \text{s.t. } & G_\theta(x(t_i),u) \leq -6V(x(t_i)) + \varepsilon, \\ & \psi_{2,\theta}(x(t_i),u) \geq c, \\ & -0.4mg \leq u \leq 0.4mg. \end{aligned} \tag{63}$$

Several modifications are made to (56) in this example. Firstly, as the equilibrium point lies outside the forward-invariant set, a stronger barrier property is needed to ensure Zeno exclusion, as explained in Remark 3.4. This is represented by the positive constant c in (63) rather than 0 in (56). Additionally, $F_{r,\theta}$ is an estimate of F_r obtained through learning, which is introduced in (63) to balance the control input and aerodynamic drag, ensuring the system maintains a constant velocity. Furthermore, a controller constraint is added in the last line of (63), following a similar approach to [12]. Finally, it is explicitly indicated that the optimization problem is solved only when an event is triggered, as denoted by $x(t_i)$. In the simulation, the values of the two parameters are set as $c = 50$ and $p = 50000$.

Now, the controller obtained from the optimization problem (63) is implemented as (6) with the DETM (35), (13), and (36), where $D(x)$ and $\|L_g V(x)\|$ are replaced by $\|\beta_\theta^h(x)\|$ and $\|\beta_\theta^V(x)\|$, respectively, and

$$\begin{aligned} & t_0 = 0, \\ & t_{i+1} = \\ & \inf_{t>t_i} \left\{ t \in \mathbb{R}_{\geq 0} \middle| \begin{array}{l} \eta(t) + \theta_h\left(\beta_h \alpha_2(\psi_1(x(t))) + \right. \\ \left. M\gamma(\Phi_1(x(t),\eta(t)),t) - L\|\beta_\theta^h\|\|e(t^-)\|\right) \leq 0 \\ \text{or } \zeta(t) + \theta_v\left(\beta_v \alpha_v(\|x(t)\|) - L\|\beta_\theta^v\|\|e(t^-)\|\right) \leq 0 \end{array} \right\}, \end{aligned}$$

and $\eta(t)$ and $\zeta(t)$ are two internal dynamic variables with

$$\dot{\eta} = -\delta_h \eta + \beta_h \alpha_2\left(\psi_1(x)\right) + M\gamma\left(\Phi_1(x,\eta),t\right) - L\|\beta_\theta^h\|\|e\|,$$

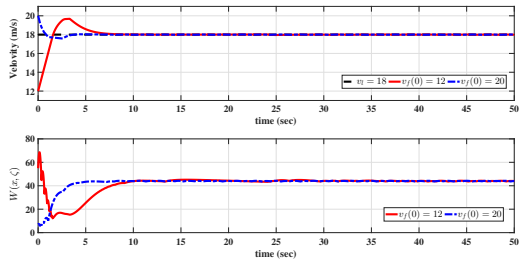

Fig. 8: Top: Velocity profiles of the lead car and the following car under different initial conditions; Bottom: Profiles of $W(x,\zeta)$ under different initial conditions.

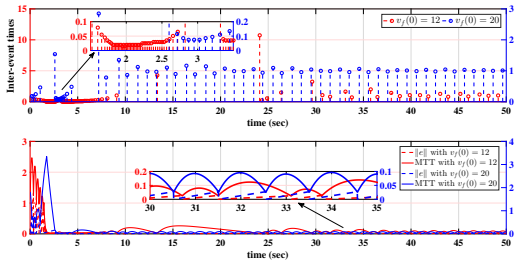

Fig. 9: Top: Inter-event time profiles with different initial velocities; Bottom: Evolution of measurement error $\|e(t)\|$ and the minimum triggering threshold (MTT) with different initial velocities.

$$\eta_0 = \psi_1(x_0),\ \forall\, t \geq t_0,$$

and

$$\dot{\zeta} = -\delta_v \zeta + \beta_v \alpha_v(\|x\|) - L\|\beta_\theta^v\|\|e\|,$$
$$\zeta_0 = 5,$$

where $\Phi_1 = \psi_1 - \eta$. The parameter values used for this implementation are as follows: $\theta_h = \theta_v = 0.05$, $\beta_h = 0.01$, $\beta_v = 0.8$, $M = 0.1$, $\delta_h = \delta_v = 1.02$, $L = 50000$, and $\gamma(\Phi_1, t) = \Phi_1 e^{-50t}$.

The simulation results are presented in Figs. 8-11 for two distinct initial conditions: $x_0 = [18, 12, 60]^T$ and $x_0 = [18, 20, 60]^T$, using a fixed time step of $\Delta t = 0.005$ $[sec]$. In Fig. 8, it is evident that the velocity of the following car converges to the lead car's velocity. Moreover, Fig. 8 indicates that the value of $W(x,\zeta)$ approaches a nonzero constant, signifying the enforcement of the safety constraint while relaxing the stability condition. Fig. 9 illustrates the absence of Zeno phenomena in the top graph. Additionally, the bottom graph displays both the measurement error $\|e(t)\|$ and the minimum triggering threshold values, as determined by the conditions outlined in (35). Fig. 10 reveals that the controller maintains a constant value within each time interval, ensuring compliance with constraint conditions. Finally, Fig. 11 displays positive values for both $h(x)$ and $\psi_1(x)$, affirming the safety of the car's velocity concerning the set $\mathscr{C}_1 \cap \mathscr{C}_2$. The effectiveness of the proposed method is thus satisfactorily demonstrated.

VII. Conclusions

This paper has investigated event-triggered and intermittent emulation of safety-critical controllers for nonlinear systems.

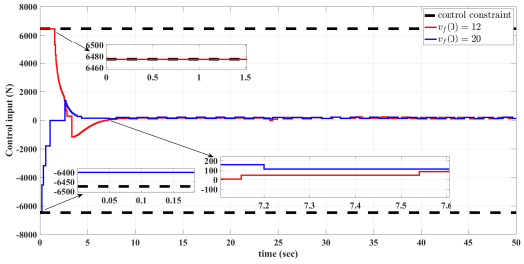

Fig. 10: Evolution of the control signal $u(t)$ satisfying the control constraint for two different initial velocities.

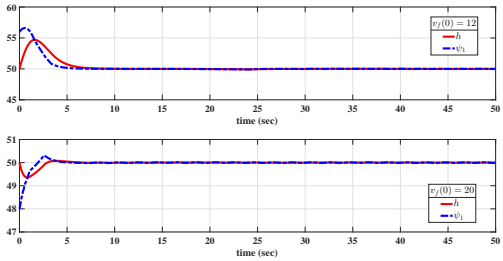

Fig. 11: Profile of $h(x)$ and $\psi_1(x)$ with different initial velocities.

Various dynamic event-triggered mechanisms have been developed to simultaneously ensure forward invariance, asymptotic convergence, and the prevention of Zeno phenomena for the safety-critical controllers constructed based on HOCBF and their resultant Lyapunov function. Additionally, we have established a supervised learning framework to handle unknown dynamics. It is anticipated that the approach developed in this paper can be applied to address safety-critical control in practical engineering problems in future work.

Acknowledgment

The authors would like to thank the associate editor and reviewers for their constructive comments and suggestions which have helped greatly improve the quality and presentation of this paper.

References

[1] F. Berkenkamp, R. Moriconi, A. P. Schoellig, and A. Krause, "Safe learning of regions of attraction for uncertain, nonlinear systems with gaussian processes," in *2016 IEEE 55th Conference, Decision and Control*, 2016, pp. 4661–4666.

[2] P. Glotfelter, J. Cortés, and M. Egerstedt, "Nonsmooth barrier functions with applications to multi-robot systems," *IEEE Control Systems Letters*, vol. 1, no. 2, pp. 310–315, 2017.

[3] N. Hovakimyan, C. Cao, E. Kharisov, E. Xargay, and I. M. Gregory, "L_1 adaptive control for safety-critical systems," *IEEE Control Systems Magazine*, vol. 31, no. 5, pp. 54–104, 2011.

[4] J. C. Knight, "Safety critical systems: Challenges and directions," in *Proceedings of the 24th International Conference on Software Engineering*, 2002, pp. 547–550.

[5] L. Wang, A. D. Ames, and M. Egerstedt, "Safety barrier certificates for collisions-free multirobot systems," *IEEE Transactions on Robotics*, vol. 33, no. 3, pp. 661–674, 2017.

[6] A. Agrawal and K. Sreenath, "Discrete control barrier functions for safety-critical control of discrete systems with application to bipedal robot navigation," *Robotics: Science and Systems*, vol. 13, 2017.

[7] T. G. Molnar, R. K. Cosner, A. W. Singletary, W. Ubellacker, and A. D. Ames, "Model-free safety-critical control for robotic systems," *IEEE Robotics and Automation Letters*, vol. 7, no. 2, pp. 944–951, 2021.

[8] G. Wu and K. Sreenath, "Safety-critical and constrained geometric control synthesis using control lyapunov and control barrier functions for systems evolving on manifolds," in *2015 American Control Conference*, 2015, pp. 2038–2044.

[9] A. D. Ames, S. Coogan, M. Egerstedt, G. Notomista, K. Sreenath, and P. Tabuada, "Control barrier functions: Theory and applications," in *2019 18th European Control Conference*, 2019, pp. 3420–3431.

[10] A. D. Ames, X. Xu, J. W. Grizzle, and P. Tabuada, "Control barrier function based quadratic programs for safety critical systems," *IEEE Transactions on Automatic Control*, vol. 62, no. 8, pp. 3861–3876, 2017.

[11] W. Xiao and C. Belta, "High order control barrier functions," *IEEE Transactions on Automatic Control*, vol. 67, no. 7, pp. 3655–3662, 2022.

[12] ——, "Control barrier functions for systems with high relative degree," in *2019 58th IEEE Conference on Decision and Control (CDC)*, 2019, pp. 474–479.

[13] W. S. Cortez, D. Oetomo, C. Manzie, and P. Choong, "Control barrier functions for mechanical systems: Theory and application to robotic grasping," *IEEE Transactions on Control Systems Technology*, vol. 29, no. 2, pp. 530–545, 2019.

[14] X. Xu, J. W. Grizzle, P. Tabuada, and A. D. Ames, "Correctness guarantees for the composition of lane keeping and adaptive cruise control," *IEEE Transactions on Automation Science and Engineering*, vol. 15, no. 3, pp. 1216–1229, 2018.

[15] A. Girard, "Dynamic triggering mechanisms for event-triggered control," *IEEE Transactions on Automatic Control*, vol. 60, no. 7, pp. 1992–1997, 2015.

[16] R. Postoyan, P. Tabuada, D. Nešić, and A. Anta, "A framework for the event triggered stabilization of nonlinear systems," *IEEE Transactions on Automatic Control*, vol. 60, no. 4, pp. 982–996, 2015.

[17] P. Tabuada, "Event-triggered real-time scheduling of stabilizing control tasks," *IEEE Transactions on Automatic Control*, vol. 52, no. 9, pp. 1680–1685, 2007.

[18] L. Long and T. Hu, "Safety-critical control and optimization of nonlinear systems based on new forms of clf-cbf-qp," *Control Theory & Applications*, vol. 39, no. 8, 2022.

[19] L. Long, F. Wang, and Z. Chen, "Robust adaptive dynamic event-triggered control of switched nonlinear systems," *IEEE Transactions on Automatic Control*, vol. 68, no. 8, pp. 4873–4887, 2023.

[20] L. Long and J. Wang, "Safety-critical dynamic event-triggered control of nonlinear systems," *Systems & Control Letters*, vol. 162, p. 105176, 2022.

[21] A. J. Taylor, P. Ong, J. Cortés, and A. D. Ames, "Safety-critical event triggered control via input-to-state safe barrier functions," *IEEE Control Systems Letters*, vol. 5, no. 3, pp. 749–754, 2021.

[22] P. Ong, G. Bahati, and A. D. Ames, "Stability and safety through event-triggered intermittent control with application to spacecraft orbit stabilization," in *2022 IEEE 61st Conference on Decision and Control (CDC)*, 2022, pp. 453–460.

[23] J. Choi, F. Castaneda, C. J. Tomlin, and S. Koushil, "Reinforcement learning for safety-critical control under model uncertainty, using control lyapunov functions and control barrier functions," *Robotics: Science and Systems*, 2020.

[24] A. J. Taylor, A. Singletary, Y. Yue, and A. D. Ames, "Learning for safety-critical control with control barrier functions," in *Proceedings of the 2nd Conference on Learning for Dynamics and Control*, 2020, pp. 708–717.

[25] W. Xiao, C. Belta, and C. G. Cassandras, "Event-triggered control for safety-critical systems with unknown dynamics," *IEEE Transactions on Automatic Control*, vol. 68, no. 7, pp. 4143–4158, 2023.

[26] ——, "Event-triggered safety-critical control for systems with unknown dynamics," in *2021 60th IEEE Conference on Decision and Control*, 2021, pp. 540–545.

[27] A. J. Taylor and A. D. Ames, "Adaptive safety with control barrier functions," in *2020 American Control Conference*, 2020, pp. 1399–1405.

[28] X. Tan, W. S. Cortez, and D. V. Dimarogonas, "High-order barrier functions: Robustness, safety, and performance-critical control," *IEEE Transactions on Automatic Control*, vol. 67, no. 6, pp. 3021–3028, 2021.

[29] M. H. Cohen and C. Belta, "High order robust adaptive control barrier functions and exponentially stabilizing adaptive control lyapunov functions," in *2022 American Control Conference (ACC)*, 2022, pp. 2233–2238.

[30] A. Isidori, *Nonlinear Control Systems*. Springer, 1995.

[31] R. Konda, A. D. Ames, and S. Coogan, "Characterizing safety: Minimal control barrier functions from scalar comparison systems," *IEEE Control Systems Letters*, vol. 5, no. 2, pp. 523–528, 2020.

[32] W. S. Cortez and D. V. Dimarogonas, "On compatibility and region of attraction for safe, stabilizing control laws," *IEEE Transactions on Automatic Control*, vol. 67, no. 9, pp. 4924–4931, 2022.

[33] P. Ong and J. Cortés, "Universal formula for smooth safe stabilization," in *2019 58th IEEE Conference on Decision and Control (CDC)*, 2019, pp. 2373–2378.

[34] H. K. Khalil, *Nonlinear systems (third edition)*. Prentice-Hall, New Jersey, 2002.

[35] C. Wang, Y. Meng, Y. Li, S. L. Smith, and J. Liu, "Learning control barrier functions with high relative degree for safety-critical control," in *2021 European Control Conference*, 2021, pp. 1459–1464.

[36] L. Gyorfi, M. Kohler, A. Krzyzak, and H. Walk, *A distribution-free theory of nonparametric regression*. Springer Science & Business Media, Berlin, 2006.

[37] M. F. Reis, A. P. Aguiar, and P. Tabuada, "Control barrier function-based quadratic programs introduce undesirable asymptotically stable equilibria," *IEEE Control Systems Letters*, vol. 5, no. 2, pp. 731–736, 2021.

[38] P. Zhao, Y. Mao, C. Tao, N. Hovakimyan, and X. Wang, "Adaptive robust quadratic programs using control lyapunov and barrier functions," in *2020 59th IEEE Conference on Decision and Control*, 2020, pp. 3353–3358.

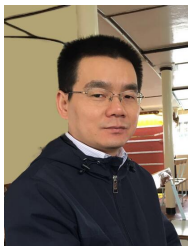

Lijun Long received the B.S. degree from Hunan Normal University, Changsha, China, in 2003, and the M.S. degree from Southwest University, Chongqing, China, in 2009, both in mathematics, and the Ph.D. degree in control theory and applications from Northeastern University, Shenyang, China, in 2013. Between July 2023 and September 2023, he was a Visiting Academic with the School of Engineering, The University of Newcastle, Callaghan, NSW 2308, Australia. He is currently a Professor with the College of Information Science and Engineering, Northeastern University, Shenyang, China. His current research interests include switched systems, nonlinear systems and control, safety-critical control, and adaptive control.

Zhongkui Zhang received the B.S. and M.S. degrees in control theory and applications from Northeastern University, Shenyang, China, in 2019 and 2023. He is currently an assistant engineer with the Shenyang Institute of Automation. His current research interests include robotics and automation, adaptive control, active disturbance rejection control, and safety-critical control.

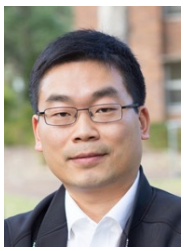

Zhiyong Chen received the B.E. degree from the University of Science and Technology of China, and the M.Phil. and Ph.D. degrees from the Chinese University of Hong Kong, in 2000, 2002 and 2005, respectively. He worked as a research associate at the University of Virginia during 2005-2006. He joined the University of Newcastle, Australia, in 2006, where he is currently a professor. He is also a Changjiang chair professor with Central South University, Changsha, China. His research interests include non-linear systems and control, biological systems, and multi-agent systems. He is/was an associate editor of Automatica, IEEE Transactions on Automatic Control and IEEE Transactions on Cybernetics.